

Tetraphenylborate Solids Stability Tests

by

D. D. Walker

Westinghouse Savannah River Company
Savannah River Site
Aiken, South Carolina 29808

DOE Contract No. DE-AC09-96SR18500

This paper was prepared in connection with work done under the above contract number with the U. S. Department of Energy. By acceptance of this paper, the publisher and/or recipient acknowledges the U. S. Government's right to retain a nonexclusive, royalty-free license in and to any copyright covering this paper, along with the right to reproduce and to authorize others to reproduce all or part of the copyrighted paper.

DISTRIBUTION OF THIS DOCUMENT IS UNLIMITED

MASTER

DISCLAIMER

Portions of this document may be illegible electronic image products. Images are produced from the best available original document.

DISCLAIMER

This report was prepared as an account of work sponsored by an agency of the United States Government. Neither the United States Government nor any agency thereof, nor any of their employees, makes any warranty, express or implied, or assumes any legal liability or responsibility for the accuracy, completeness, or usefulness of any information, apparatus, product, or process disclosed, or represents that its use would not infringe privately owned rights. Reference herein to any specific commercial product, process, or service by trade name, trademark, manufacturer, or otherwise does not necessarily constitute or imply its endorsement, recommendation, or favoring by the United States Government or any agency thereof. The views and opinions of authors expressed herein do not necessarily state or reflect those of the United States Government or any agency thereof.

This report has been reproduced directly from the best available copy.

Available to DOE and DOE contractors from the Office of Scientific and Technical Information, P.O. Box 62, Oak Ridge, TN 37831; prices available from (615) 576-8401.

Available to the public from the National Technical Information Service, U.S. Department of Commerce, 5285 Port Royal Road, Springfield, VA 22161.

RECORDS ADMINISTRATION



ABLP

TETRAPHENYLBORATE SOLIDS STABILITY TESTS (U)

D. D. Walker

Publication Date: June 25, 1997

Westinghouse Savannah River Company
Savannah River Technology Center
Aiken, SC 29808



Tetraphenylborate Solids Stability Tests (U)

Author

Darrel D. Walker

6/25/97

D. D. Walker, Waste Processing Technology Date

Design Check

R. A. Peterson

6/25/97

R. A. Peterson, Waste Processing Technology Date
(per Manual E7, Procedure 2.40)

Approvals

Samuel D. Fink

6/25/97

S. D. Fink, Level 4 Manager
Waste Processing Technology

Date

W. L. Tamosaitis

7/22/97

W. L. Tamosaitis, Level 3 Manager
Waste Processing Technology

Date

J. T. Carter

7/12/97

J. T. Carter
In-Tank Precipitation Flow Sheet Team Leader

Date

M. J. Montini

7/14/97

M. J. Montini, Deputy Manager
ITP/ESP Engineering

Date

CONTENTS

SUMMARY.....	5
INTRODUCTION.....	6
DISCUSSION.....	7
Test Matrix and Conditions.....	7
Radioactive Experiments.....	7
Simulant Experiments.....	8
Test Results.....	10
Appearance of Cs-137 and K ⁺	13
Temperature Dependence.....	14
Potassium and Cs-137 Correlation.....	14
Other Observations.....	16
Decomposition Model.....	16
Comparison of Models.....	20
Model Fit to Data.....	22
Radioactive Experiments.....	22
Simulant Experiments.....	22
Tank 48H Data.....	24
Previous Laboratory Tests.....	27
Discussion of Modeling Results.....	29
RECOMMENDATIONS FOR FURTHER TESTING.....	30
REFERENCES.....	31
APPENDIX A: Experimental.....	32
APPENDIX B: G Value for Appearance of K ⁺ from Radiolysis.....	43
APPENDIX C: Calculation of K ₁ and K ₂ for Decom- position Model.....	45

TETRAPHENYLBORATE SOLIDS STABILITY TESTS (U)

By D. D. WALKER

SUMMARY

Tetraphenylborate solids are a potentially large source of benzene in the slurries produced in the In-Tank Precipitation (ITP) process. The stability of the solids is an important consideration in the safety analysis of the process and we desire an understanding of the factors that influence the rate of conversion of the solids to benzene. This report discusses current testing of the stability of tetraphenylborate solids. The appearance of soluble potassium and cesium ions indicate the loss of tetraphenylborate solids (KTPB and CsTPB). The experiments measured rates of increase in soluble potassium and cesium following the loss of tetraphenylborate in radioactive waste and simulant slurries containing potential transition metal catalysts. The test results indicate the following.

- Potassium and Cs-137 concentrations in solution become measurable when the excess sodium tetraphenylborate concentration drops below 50 mg/L.
 - This result agrees with expectations from the solubility of KTPB and CsTPB.
- The rate of appearance of soluble Cs-137 and potassium increases with temperature. The process should avoid temperatures of 64 °C or higher.
 - Below 45°C and at current Tank 48H radionuclide levels, the rate remains slow and corresponds to loss of 0.05 wt % precipitate solids per year.
 - At temperatures of 64 and 70°C, the rate increases and corresponds to loss of all of the precipitate in less than one year assuming the rate persists. Actual losses during 20-day experiments were approximately 0.28 wt % precipitate solids (out of 4 wt % solids in the slurry).
 - The potential for rapid loss of precipitate between 45 and 64 °C is not clearly defined by the completed tests. Additional studies are recommended in this temperature range.
 - Personnel can study the reaction with non-radioactive simulants by measuring potassium concentrations.

- Simulant responses were qualitatively similar to radioactive waste, but with rates typically slower under similar temperature conditions.
 - A radiation-induced decomposition mechanism was known previously, but radiation is not a necessary condition for the appearance of soluble potassium and Cs-137.
- The ratio of Cs-137 to potassium in radioactive waste trends toward the ratio of the solubility products for CsTPB and KTPB.
 - This suggests that solubility equilibrium influences the soluble potassium and Cs-137 concentrations.

The author developed a dual mechanism model that predicts potassium and cesium concentrations. The model includes a radiolytic decomposition mechanism based on the radiation dose to the solids and catalytic decomposition mechanism based on the concentration of soluble tetraphenylborate ion. Application of this model to the available data provides the following results.

- The model predicts Tank 48H post-1983 and post-PVT-1 behavior accurately when including the effect of K^+/Cs^+ ratio on the solubility of CsTPB.
- The model over predicts K^+ and Cs^+ in some laboratory experiments and in Tank 48H following the 1995 Batch 1.
- The model does not predict the first day's increase in Cs-137 in one previously reported test in which a large change occurred, but predicts the subsequent rate of increase in cesium.
- The model does not predict or bound the accelerating rate observed in four experiments at higher temperatures.

These results indicate that the two mechanism model adequately predicts or bounds the behavior of radioactive waste and simulant slurries at lower temperatures ($\leq 45^{\circ}\text{C}$) within the limited experimental conditions tested. However, the substantial under prediction of the model at higher temperatures suggests a significant additional reaction mechanism contributing to the decomposition.

INTRODUCTION

During the Savannah River Technology Center's (SRTC) preparations for the Tank 48H Process Verification Test, Phase 1 (PVT-1), researchers performed several experiments in the Shielded Cells using slurries from Tank 48H. Two

experiments showed an increase in soluble Cs-137 following the decomposition of the excess sodium tetraphenylborate (NaTPB).¹ The rate and magnitude of the increase in Cs-137 exceeded observations of Tank 48H.²⁻³ Two interpretations have been suggested. First, the increase may reflect increases in the solubility of potassium and cesium tetraphenylborate (KTPB and CsTPB) as the solution concentration of tetraphenylborate ion (TPB⁻) decreased due to decomposition. As TPB⁻ decreased in solution, KTPB and CsTPB dissolved to maintain saturation with respect to K⁺, Cs⁺ and TPB⁻. The second interpretation suggests K⁺ and Cs⁺ increased in solution by a direct chemical attack or decomposition of the tetraphenylborate solid phase. This interpretation raises concerns because of the potential benzene generation term which would result if all of the precipitated KTPB and CsTPB solids decomposed. Personnel must understand the factors governing the rate of release of soluble cesium from the precipitate to fully develop the safety and operational bases for the facility.

Previous testing focused on the loss of TPB⁻ and experiments terminated before Cs⁺ and K⁺ began to increase. Only a small amount of reliable data exists that measured the increase in Cs-137 and K⁺ following loss of TPB⁻. Testing the two postulates requires additional measurements. Personnel designed a set of experiments to measure the effects of temperature, weight percentage solids, and excess TPB⁻ using slurry samples from Tank 48H. To provide data for Late Wash operations, washed samples of the Tank 48H slurry were tested.

In an additional activity, researchers prepared and tested non-radioactive simulated waste slurry to determine if it responds similarly to Tank 48H slurries. These experiments attempted to show the adequacy of using simulants rather than radioactive waste in subsequent experiments.

The results of all experiments provide data for modeling the increase in Cs-137. A mathematical model that predicts the rate of increase in Cs-137 and K⁺ would demonstrate an adequate understanding of the factors that cause Cs-137 and K⁺ increases in Tank 48H and laboratory experiments.

DISCUSSION

Test Matrix and Conditions

Radioactive Experiments

Experiments 1 through 6 used Tank 48H slurry samples in the Shielded Cells Facility. These experiments studied four variables: temperature (40, 50, and 65 °C), weight percentage solids (1 and 4 wt %), initial TPB⁻ concentration (target: 100 and 400 mg/L), and salt concentration (0.5, 1.5, and 3.0 molar Na⁺). Table I shows the test matrix with targeted

values. The four experiments at 3 molar Na^+ provide data on Tank 48H at the current conditions. The diluted samples (0.5 and 1.5 M Na^+) at higher temperature (65 °C) provide information about Late Wash conditions. The actual experimental conditions differed slightly, particularly in the initial TPB^- concentrations and the initial sodium ion concentrations.

Researchers combined slurry samples taken from Tank 48H during June, July, and August to form a large batch of approximately 2 wt % slurry. They then adjusted this composite to produce the slurries used in the experiments. Appendix A gives details of the slurry origin and preparation.

Personnel placed the slurries in carbon steel containers, sealed under air, and placed into an oven at the test temperature. The samples were not continuously stirred, but were mixed prior to sampling. The first samples were taken after four days, followed by subsequent sampling once or twice a week depending on the apparent rate of change in the sample.

The researchers filtered samples with the filtrate analyzed for Cs-137, K^+ , NaTPB , intermediate organic compounds, and phenol. Figure 1 graphs the results with numerical values listed in Appendix A.

Simulant Experiments

Experiments 7 through 12 used non-radioactive simulants of the Tank 48H slurry. These experiments examined temperature and initial NaTPB concentration as variables. Table II lists the targeted initial conditions for these experiments. The slurry composition simulated current Tank 48H. Personnel prepared the slurries by the following steps.

- Precipitated KTPB solids in salt solution to obtain a 4 wt % slurry.
- Added potential catalyst components (sludge, monosodium titanate, soluble minor metals, and diphenylmercury).
- Irradiated slurry and catalyst to a total dose of 5 Mrad.

For Experiments 7, 8 and 12, personnel performed the following steps.

- Spiked the slurry to achieve 1.7 wt % NaTPB (corresponding to approximately the ratio of NaTPB to KTPB in Tank 48H during first batch operations).
- Heated the slurries at 70°C for 25 days to decompose the majority of the NaTPB .
- Adjusted the NaTPB concentration to obtain the targeted TPB^- concentration.

TABLE I. Test Matrix for Radioactive Experiments*

<u>Experiment</u>	Temp. (°C)	Initial		
		[Na ⁺] (M)	Solids (wt %)	[TPB ⁻] (mM)
1	40	3.0	1	0.29
2	40	3.0	4	1.2
3	50	3.0	1	1.2
4	50	3.0	4	0.29
5	65	0.5	4	1.2
6	65	1.5	4	1.2

*Targeted values. See Table III for actual conditions.

TABLE II. Test Matrix for Simulant Experiments*

<u>Experiment</u>	Temp. (°C)	Initial		
		[Na ⁺] (M)	Solids (wt %)	[TPB ⁻] (mM)
7	40	3.0	4	0.29
8	40	3.0	4	1.2
9	40	3.0	4	0.29
10	40	3.0	4	1.2
11	50	3.0	4	0.29
12	70	3.0	4	0.29

*Targeted values. See Table III for actual conditions.

TABLE III. Summary of Test Conditions and Results

	Experiment	Temp. (°C)	[Na ⁺] (molar)	Solids (wt %)	Initial NaTPB (mimolar)	Cs-137 Rate* (nCi/mL/day)	K+ Rate* (mg/L/day)
Real Waste	1	40	2.7	0.8	0.096	13	0.15
	2	40	2.7	4.7	1.06	7	0.11
	3	50	2.7	0.8	0.81	3	0.22
	4	50	2.7	4.7	0.38	130	1.3††
	5	64	0.4	4.1	1.84	4800	60
	6	64	0.9	4.8	1.53	15000	130
Simulant	7	40	3.0	4.0	<.03	†	<.1
	8	40	3.0	4.0	<.03	†	<.1
	9	40	3.0	4.0	0.73	†	**
	10	40	3.0	4.0	1.08	†	**
	11	49	3.0	4.0	0.67	†	2
	12	70	3.0	4.0	0.28	†	40

*The listed rates of increase in Cs-137 and K⁺ are the maximum slope observed in tests
**Soluble NaTPB was not completely consumed before the end of the test, therefore no increase
potassium was expected or measured.
†Cs-137 was not present in the simulant tests.
††Calculated from the Cs-137 rate using a Cs/K ratio of 100 Ci/kg.

For Experiments 9 and 10, the slurry preparation did not include the NaTPB addition and 70° heat treatment. After irradiation, personnel performed the following step.

- Adjusted the NaTPB to obtain the targeted TPP⁻ concentration.

In most cases the observed TPP⁻ concentration at the beginning of the experiment was not close to the targeted concentration. Appendix A gives further details of the preparation.

Researchers placed the slurries in 150-mL glass serum vials, sealed under nitrogen, and placed into ovens at the test temperature. The samples received mixing only prior to sampling. Personnel filtered samples and analyzed for the same components as the radioactive experiments with the exception of Cs-137. Figure 2 graphs the results with the numerical values listed in Appendix A.

Test Results

The appearance of soluble potassium and cesium ions was used as a measure of the loss of tetraphenylborate solids (KTPB and CsTPB). Researchers measured the rates of increase in soluble potassium and cesium in radioactive and simulant slurries containing potential transition metal catalysts. In most experiments, researchers measured the loss of TPP⁻ prior to the appearance of measurable amounts of soluble potassium and cesium.

Table III summarizes the experimental results from which the following conclusions are derived.

- Potassium and Cs-137 concentrations in solution become measurable when the measured sodium tetraphenylborate concentration in solution drops below 50 mg/L.
- The rate of appearance of soluble Cs-137 and potassium increases with temperature.
 - Below 45°C and at current Tank 48H radionuclide levels, the rate remains slow and corresponds to loss of 0.05 wt % precipitate solids per year.
 - At temperatures of 65 and 70°C, the rate increases and corresponds to loss of all of the precipitate in less than one year assuming the rate persists. Actual losses during 20-day experiments were approximately 0.28 wt % precipitate solids (out of 4 wt % solids in the slurry).
 - Personnel can study the reaction with non-radioactive simulants by measuring potassium concentrations.

FIGURE 1. Results of Radioactive Experiments

Notes: The vertical and horizontal scales on these graphs are not all the same. Use care when comparing different experiments. Soluble tetraphenylborate concentrations are shown as NaTPB (mg/L). Thus, 342 mg/L equal 0.001 M TPB.

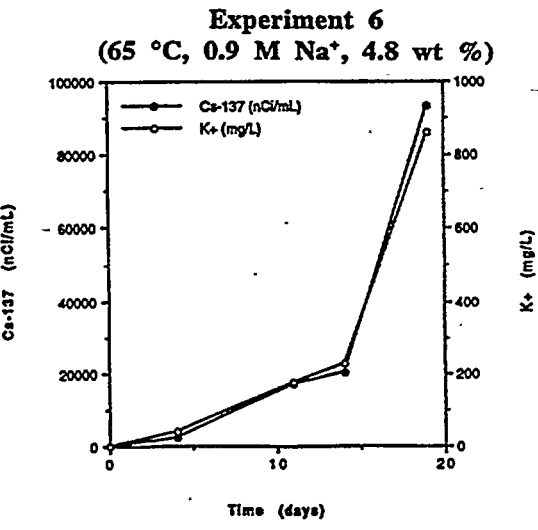
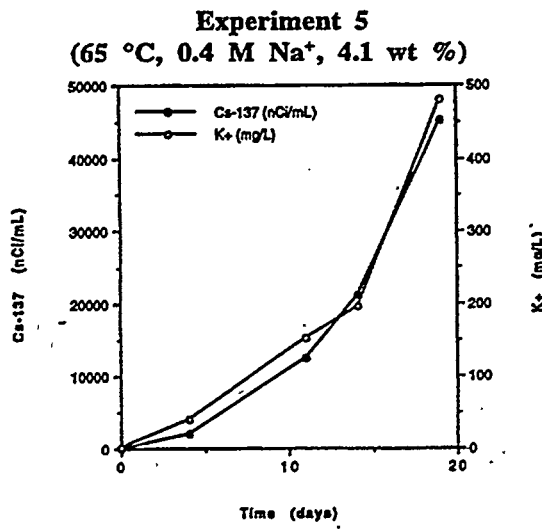
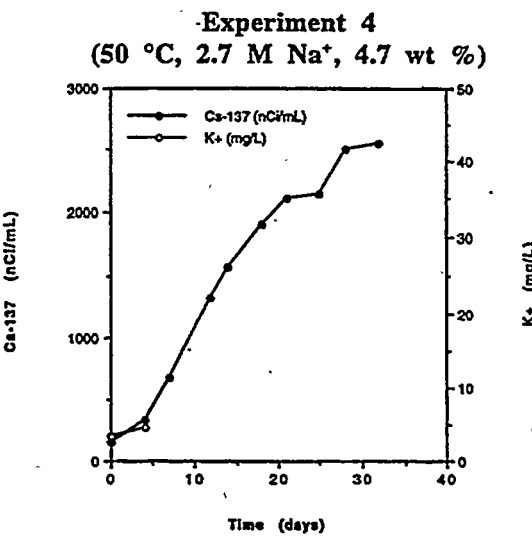
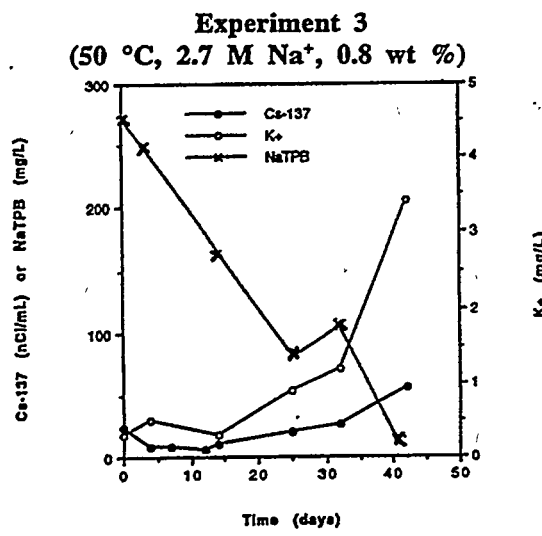
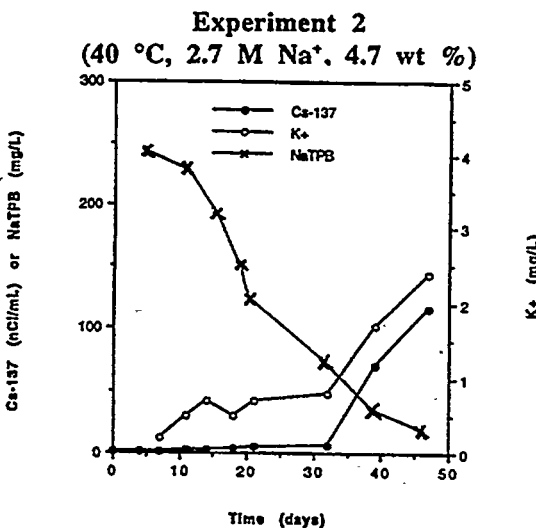
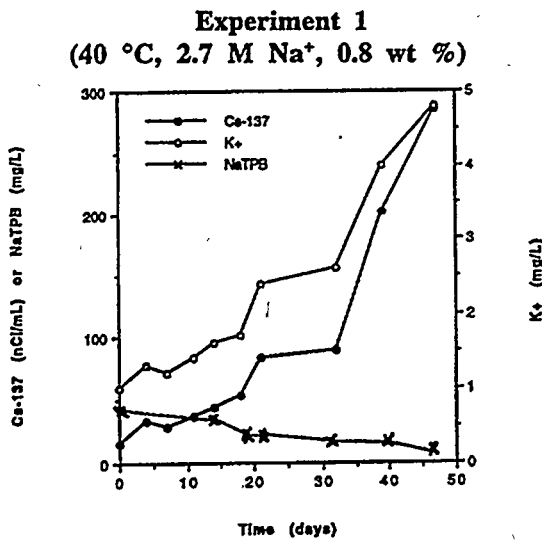
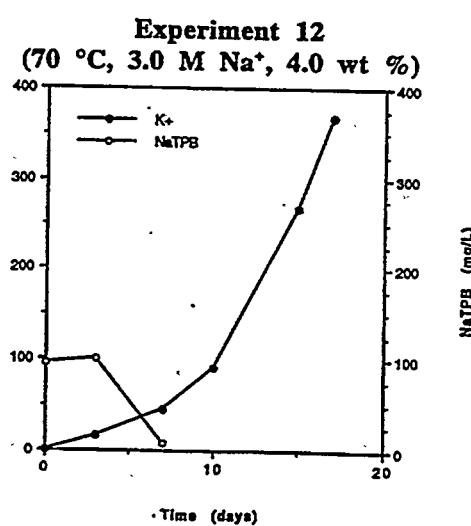
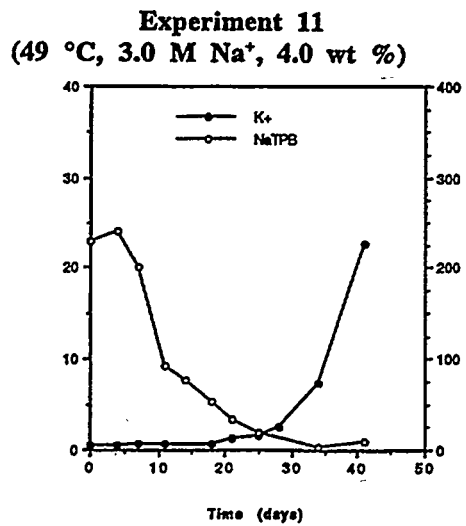
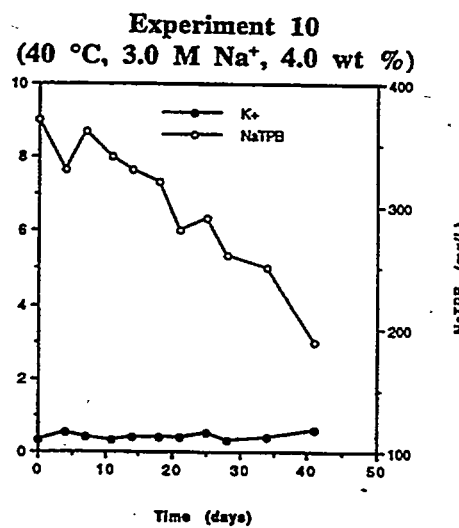
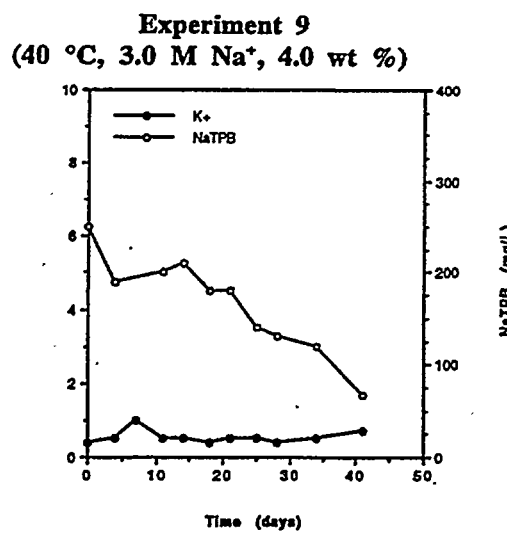
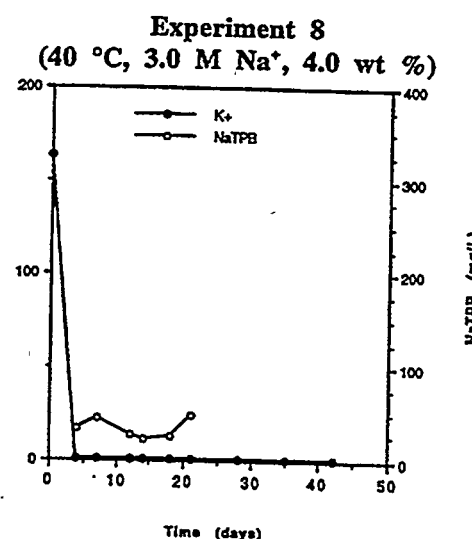
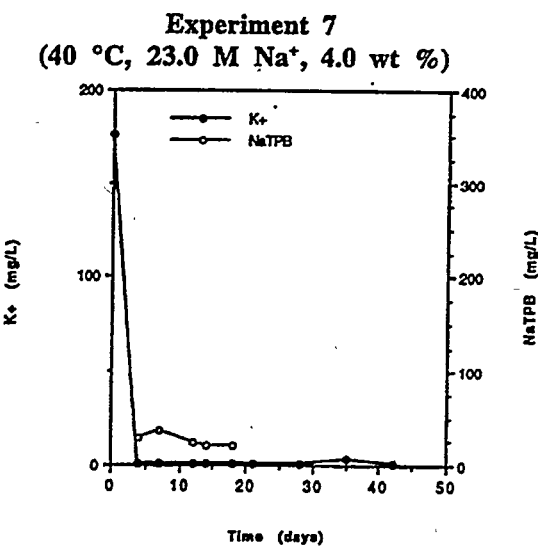


FIGURE 2. Results of Simulant Experiments

Notes: The vertical and horizontal scales on these graphs are not all the same. Use care when comparing different experiments. Soluble tetrphenylborate concentrations are shown as NaTPB (mg/L). Thus, 342 mg/L equal 0.001 M TPB.



- Simulant responses were qualitatively similar to radioactive waste, but rates were typically slower under similar temperature conditions.
 - A radiation-induced decomposition mechanism was known previously, but radiation does not appear a necessary condition for the appearance of soluble potassium and Cs-137.
- The ratio of Cs-137 to potassium in radioactive experiments trends toward the ratio of the solubility products for CsTPB and KTPB.
 - This suggests that solubility equilibrium influences the soluble potassium and Cs-137 concentrations.

Appearance of Cs-137 and K⁺

In laboratory experiments, cesium and potassium ions appear as soluble components when the TPB⁻ ion concentration drops below approximately 0.15 millimolar (0.15 mmolar or 50 mg/L). This response results from the low but finite solubility of KTPB and CsTPB. However, the concentrations of soluble K⁺ and Cs-137 are slightly lower than calculated from solubility measurements of pure KTPB and CsTPB. This deviation may reflect slow dissolution of Cs⁺ and K⁺ or, in the case of cesium, result from an effect of precipitating in the presence of potassium (producing a mixed crystal of lower solubility).⁴

The graphs in Figure 2 show the changes in soluble NaTPB and potassium in the simulant experiments. In Experiments 9 and 10, the potassium concentration never exceeded 1 mg/L because the soluble NaTPB did not decompose to less than 50 mg/L. In Experiments 11 and 12, the appearance of soluble K⁺ begins when the NaTPB concentration drops.

Potassium did not increase in Experiments 7 and 8 even though the soluble NaTPB concentration dropped below the 10 mg/L detection limit. The failure of KTPB to dissolve could reflect slow dissolution kinetics of KTPB in the unstirred samples, or slow dissolution of NaTPB solids. The presence of NaTPB solids is suggested by the drop in potassium between the initial and subsequent samples.

Figure 1 includes soluble NaTPB for the first three radioactive experiments. The Cs-137 and potassium ion did not increase significantly until the soluble tetraphenylborate concentration dropped below 0.15 mmolar. This behavior also occurred in Tank 48H during the Process Verification Test, Phase 1.⁵

Temperature Dependence

Temperature is the most obvious effect on the rate of increase in soluble potassium and cesium. In the temperature range studied (40 to 70 °C), the rates vary by three orders of magnitude. Table III lists the rates of increase near the end of each experiment. The table omits two tests (Experiments 9 and 10) since the NaTPB did not completely decompose so no measure of the rate of increase in potassium exists.

At or below 45°C, the rate of increase in Cs-137 and potassium remains slow. If these rates persisted for a year, only 0.05 wt % KTPB would decompose (about 1% of the tetrphenylborate solids in a 5 wt % KTPB slurry, or 2% of the current Tank 48H solids). This decomposition is less than the 1 wt % KTPB annual loss from radiolytic decomposition expected in the ITP process⁶ and does not pose a significant concern.

At higher temperatures (64 and 70°C), the Cs-137 and potassium rates increase rapidly and would lead to complete decomposition of the solids in less than a year. The experiments showing the high reaction rates (5, 6, and 12) terminated after 20 days when approximately 3% to 7% of the solids decomposed. This rapid reaction occurred in both radioactive and simulant experiments. The process should clearly avoid this temperature range.

These experiments do not clearly define the potential for a rapid reaction between 45 and 64°C. Experiment 11 at 49 °C (Figure 2) shows a sharp upward trend at the end of the test. Although the rate at the end of this experiment remained acceptable (2 mg/L/day, or about 12% of a 5 wt % slurry per year), the experiment likely terminated before reaching the maximum rate. Under similar conditions with radioactive waste, Experiment 4 at 50°C (Figure 1) did not appear to accelerate at the end of the test. One can calculate an approximate rate for potassium from the cesium data and the observed cesium/potassium ratio in other experiments. The rate so obtained in Experiment 4 proves comparable to Experiment 11. The rate in Experiment 3 (at 50°C) remains slow, probably due to the delay in consuming the high initial level of NaTPB until the end of the test. Hence, Experiment 3 likely stopped before achieving the maximum rate of increase in Cs-137.

Potassium and Cesium-137 Correlation

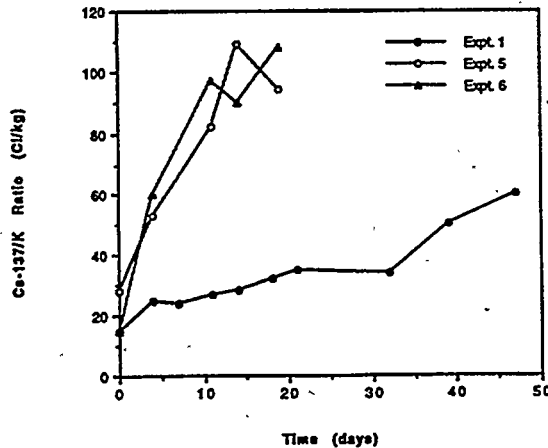
The graphs of the radioactive experiments (Figure 1) indicate that Cs-137 and potassium begin to increase in solution at approximately the same time. This correlation agrees with most explanations of the process chemistry. Comparing the graphs for radioactive experiments to the simulant

experiments indicate that the two systems respond qualitatively similarly. A comparison of rates listed in Table III suggests approximate quantitative agreement as well. At each temperature, the rates in the two systems are of the same order of magnitude, although the simulants are consistently slower. These observations suggest that the reaction will occur in the absence of radiation and that simulant experiments are adequate for further studies.

The value of the ratio of Cs-137/K can distinguish between some hypotheses about the reaction. Possible ratios between Cs-137 and K⁺ include (1) the ratio in which they exist in the tank, (2) the ratio of the solubility products of KTPB and CsTPB, and (3) the ratio of the rate at which the two compounds decompose. A prior report estimated the ratio in which they exist in the tank (total for both solids and soluble) as 180 Ci Cs-137 per kilogram of potassium.⁴ The ratio of the solubility products for KTPB and CsTPB varies with temperature and salt concentration, but measures approximately 130 Ci/kg for conditions relevant to this study. No evidence exists for separate rates for the decomposition of the two compounds. Personnel postulated that CsTPB may be more sensitive to decomposition, thus explaining the results in the previous test -- Test #2 of Ref. 1 -- that showed a large increase in Cs-137 in solution. If this sensitivity existed, the Cs-137/K ratio would exceed the bulk average, 180 Ci/kg.

The Cs-137/K ratios observed in the experiments are most consistent with the solubility product ratio of CsTPB and KTPB. The measured Cs-137/K ratio changes systematically, starting low (15-30 Ci/kg) and increasing steadily to values as high as 108 Ci/kg. Figure 3 graphs these changes for Experiments 1, 5, and 6 which offer the most data. The

FIGURE 3. Cs-137/Potassium Ratio Observed in Radioactive Experiments



results for Experiments 5 and 6 suggest that the rate changes slowly, possibly leveling off near the ratio of the solubility products. However, the reason why solubility controls the ratio in fast reactions (Experiments 5 and 6) and not in a slower reaction (Experiment 1) remains unclear. The low ratio most likely reflects the effect of the Cs/K ratio on the apparent solubility of CsTPB.⁵ The solubility ratio used above used the K_{sp} 's for the pure phases. Recent solubility experiments indicate that cesium is less soluble when precipitated in the presence of potassium. Another explanation leading to low ratios assumes that the system has not reached equilibrium and that KTPB dissolves faster. The higher relative rates of dissolution for KTPB seem reasonable since much more KTPB is present with correspondingly more surface area which would increase its rate of dissolution.

Other Observations

The statistical design of Experiments 1 through 4 allows measurement of the primary effects of temperature, initial NaTPB concentration, and solids concentration. However, Experiment 3 contained a high initial NaTPB concentration slowing the increase in Cs-137 and K⁺ until late in the experiment. As a result, the measured response may be low because the reaction never fully developed. If the analysis disregards the result for Experiment 3, the results of the remaining experiments are insufficient to draw conclusions. If the analysis includes Experiment 3, then the results indicate that increasing the temperature or the weight percentage solids increases the response (i.e., Cs-137 and potassium rates of increase), whereas high initial NaTPB decreases the response. The latter result may simply reflect a delay in the onset of the increase in Cs-137 and K⁺ caused by a high initial NaTPB concentration. The interest in the initial TPB⁻ concentration was based on speculation that intermediate decomposition compounds might play a role in the reaction.⁶ Thus higher initial TPB⁻ might affect the eventual rate by generating higher concentrations of intermediates.

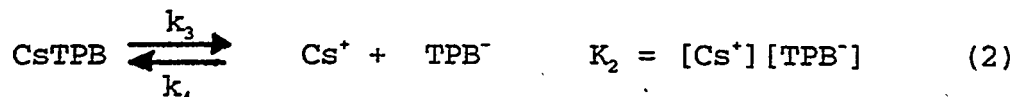
A comparison of the results of Experiments 5 and 6 at two different sodium ion concentrations suggest that the reaction rate is faster at the higher sodium concentration. This agrees with observations from tests to determine the catalysts responsible for the degradation of soluble TPB⁻.⁷

Decomposition Model

The author modeled the appearance of soluble K⁺ and Cs⁺ from the decomposition of tetraphenylborate slurries as the sum of two reaction mechanisms (catalytic and radiolytic). Application of this model to Tank 48H and scoping tests yields the following conclusions.

- The model predicts post-1983 and post-PVT-1 behavior accurately with slight modifications to the solubility of CsTPB.
- The model over predicts K^+ and Cs^+ following the 1995 Batch 1.
- The model predicts closely or over predicts results from low temperature experiments ($\leq 45^\circ C$), both simulated and Tank 48H slurries.
- The model does not predict the first day's jump in Test 2 of Ref. 1; but predicts the subsequent rate of increase in Cs-137.
- The model does not predict the accelerating rate observed in four experiments at 50, 65, and $70^\circ C$.

The catalytic mechanism assumes decomposition of soluble TPB^- . This mechanism includes instantaneous dissolution of KTPB and CsTPB to meet the solubility limits for K^+ , Cs^+ , and TPB^- in solution. The decomposition step depends on the soluble TPB^- concentration. The appropriate equations for this mechanism are



The k_x denote rates of dissolution and precipitation. This mechanism assumes the slurry always satisfies the equilibrium solubility conditions (Equations 1 and 2). To simplify the equations the author omitted the activity coefficients in K_1 and K_2 . Previous work⁷ measured the solubility products (K_{sp}) for KTPB and CsTPB and related these to K_1 and K_2 by the following equations.

$$KTPB: \quad K_1 = \frac{K_{sp}(KTPB)}{\gamma_{K^+} \gamma_{TPB^-}} \quad (4)$$

$$CsTPB: \quad K_2 = \frac{K_{sp}(CsTPB)}{\gamma_{Cs^+} \gamma_{TPB^-}} \quad (5)$$

Appendix C lists the values for K_1 and K_2 .

The second mechanism involves radiolytic degradation of the solids. This mechanism incorporates the dose rate to solid and a G value for appearance of K^+ in solution due to

breakdown of the solids. The following equation describes the appearance of K^+ .

$$\frac{d[K^+]}{dt} = \frac{G D}{A V} \quad (6)$$

where G represents the G value (atoms/100 eV), D denotes the dose rate (eV/sec), V reflects the volume of liquid in which the K^+ dissolves (L), and A stands for Avogadro's number (atoms/mole). Appendix B describes the experiment that measured the G value.

One can solve the equations for each mechanism separately to produce models for individual mechanisms, or in combination to yield a solution for the dual mechanism. The following differential equations describe the appearance of potassium and cesium from each mechanism.

Catalytic Mechanism.

$$\frac{d[K^+]}{dt} = k_1 - k_2 \quad \frac{d[Cs^+]}{dt} = k_3 - k_4$$

$$\frac{d[TPB^-]}{dt} = (k_1 - k_2) + (k_3 - k_4) - k[TPB^-]$$

Combining and rearranging these yields the following equation.

$$\frac{d[K^+]}{dt} + \frac{d[Cs^+]}{dt} - \frac{d[TPB^-]}{dt} = k[TPB^-]$$

Radiolytic Mechanism.

$$\frac{d[K^+]}{dt} = k_1 - k_2 + \frac{(1-a)GD}{AV} \quad \frac{d[Cs^+]}{dt} = k_3 - k_4 + \frac{aGD}{AV}$$

$$\frac{d[TPB^-]}{dt} = (k_1 - k_2) + (k_3 - k_4)$$

Combining and rearranging these yields the following equation.

$$\frac{d[K^+]}{dt} + \frac{d[Cs^+]}{dt} - \frac{d[TPB^-]}{dt} = \frac{GD}{AV}$$

Catalytic and Radiolytic Mechanisms.

$$\frac{d[K^+]}{dt} = k_1 - k_2 + \frac{(1-a)GD}{AV} \quad \frac{d[Cs^+]}{dt} = k_3 - k_4 + \frac{aGD}{AV}$$

$$\frac{d[TPB^-]}{dt} = (k_1 - k_2) + (k_3 - k_4) - k[TPB^-]$$

where a = the mole fraction of CsTPB in the solids.

Combining and rearranging these yields the following equation.

$$\frac{d[K^+]}{dt} + \frac{d[Cs^+]}{dt} - \frac{d[TPB^-]}{dt} = \frac{GD}{AV} + k[TPB^-]$$

One may solve each of these equations for $d[K^+]/dt$ by substituting relationships obtained from the solubility product equations. Integrating and using the boundary condition that $[K^+] = [K^+]$, when $t = 0$ yields the solutions listed in Table IV.

The assumption that the K^+ , Cs^+ and TPB^- concentrations always satisfy the solubility product equations forces the ratio of K^+ to Cs^+ in solution to always equal the ratio of their solubility products. Thus, one may easily calculate the Cs-137 activity from the potassium concentration knowing the ratio of Cs-137 to total cesium. For the current Tank 48H composition, Cs-137 comprises

Table IV. Solutions to Model Equations

Catalytic Mechanism

$$t = \frac{1}{k} \ln \left(\frac{[K^+]}{[K^+]_0} \right) + \frac{(1 + K_2/K_1)}{2kK_1} ([K^+]^2 - [K^+]_0^2)$$

Radiolysis Mechanism

$$t = \frac{(1 + K_2/K_1)}{(GD/AV)} ([K^+] - [K^+]_0) - \frac{K_1}{(GD/AV)} \left(\frac{1}{[K^+]} - \frac{1}{[K^+]_0} \right)$$

Catalytic and Radiolysis Mechanisms

$$t = \frac{1}{k} \ln \left(\frac{[K^+]}{[K^+]_0} \right) + \frac{(1 + K_2/K_1)}{(GD/AV)} ([K^+] - [K^+]_0) - \left(\frac{k(K_1 + K_2)}{(GD/AV)} + \frac{1}{k} \right) \ln \left(\frac{(GD/AV)[K^+]}{(GD/AV)[K^+]_0} + \frac{KK_1}{(GD/AV)[K^+]_0} \right)$$

where

t = elapsed time (h)

k = rate constant for catalytic loss of TPB^- (h^{-1})

K_1 = solubility product for $KTPB$ (molar²)

K_2 = solubility product for $CsTPB$ (molar²)

G = G value for appearance of K^+ from radiolysis (molecules/eV)

D = radiation dose rate (eV/h)

A = Avogadro's number (6.022E23 molecules/mole)

V = solution volume (L)

$[K^+]$ = concentration of potassium ion at time t (molar)

$[K^+]_0$ = concentration of potassium ion at $t = 0$ (molar)

29 atom percent of the total cesium. Given a potassium concentration, one calculates the corresponding Cs-137 activity from the following equation.

$$\text{Cs-137 (nCi/mL)} = [\text{K}^+] \left(\frac{K_2}{K_1} \right) \left(\frac{.29 \text{ mole Cs-137}}{\text{mole Cs}} \right) \left(\frac{1.19E13 \text{ nCi}}{\text{mole Cs-137}} \right) \left(\frac{1 \text{ L}}{1E3 \text{ mL}} \right)$$

where $[\text{K}^+] = \text{K}^+$ concentration (molar)

The specific activity for Cs-137 (1.19E13 nCi/mole), a physical constant, comes from reference sources or by calculation from the half life.

Comparison of Models

Figure 4 gives a comparison of the three models. The figure lists the conditions chosen for the comparison; these correspond to a possible Tank 48H condition. The plot gives the soluble potassium concentration, but the response for Cs-137 differs only by a constant factor determined by the solubility product and ratio of Cs-137 to total cesium.

The catalytic reaction is moderately fast initially when the concentration of TPB^- is appreciable. However, the rate of this reaction rapidly decreases with consumption of TPB^- . This response typifies this model: the rate of increase will slow with time and become almost flat. In the radiolytic reaction, the increase in K^+ delays for about 100 days as radiolysis decomposes enough KTPB solids to precipitate the TPB^- in solution. The delay time depends on the initial TPB^- concentration and dose rate (or, equivalently, the curies of Cs-137 in the tank). The final slope depends on the dose rate only. Variations in the G value will have minor effects on the response curve. In the combined model, potassium increases much earlier because of the combined effects of the two mechanisms. Initially, the catalytic reaction dominates and decomposes the TPB^- . Subsequently, the radiolytic reaction dominates and determines the slope of the response curve.

Figure 5 shows the effects of changes in certain parameters in the combined model. Increasing the rate of the catalytic reaction rapidly decomposes the soluble TPB^- , but the eventual slope of the line remains relatively unchanged. Increasing the initial soluble TPB^- concentration has the obvious effect of delaying the rise in soluble potassium, however the delay lasts only a few days. Lowering the dose rate delays the rise in the potassium concentration slightly, with the eventual slope changed by a factor of 1/2.

FIGURE 4. Comparison of Three Models

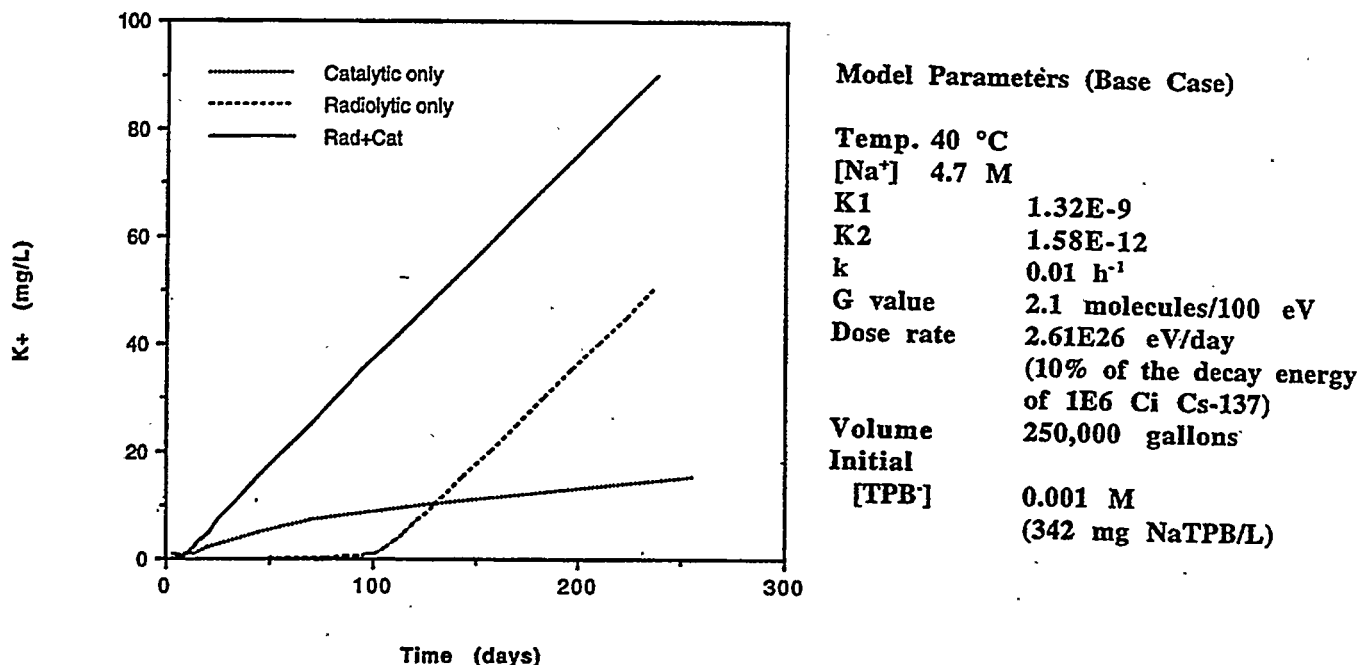
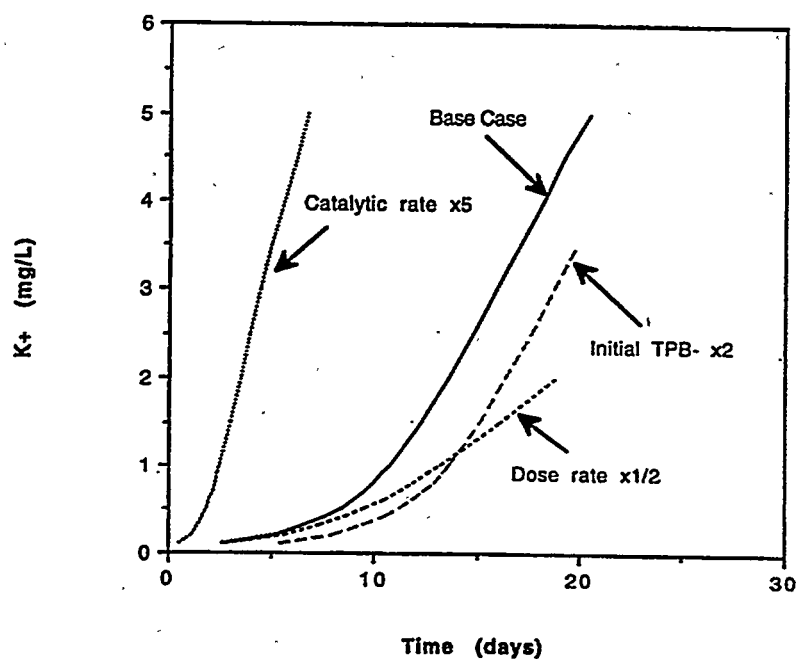


FIGURE 5. Effects of Changes in Parameters on Combined Model



Model Fit to Data

The author used the model to fit the data from the laboratory experiments and Tank 48H. The values for the parameters in the model derived from the following methods.

Solubility product constants for KTPB and CsTPB.

The solubility products depend on temperature and ionic strength (sodium ion concentration). Appendix C lists the values used from Reference 7.

Catalytic rate constant (k). The value for this constant results from fitting the data for loss of TPB⁻ obtained at the beginning of each experiment. For Tank 48H, the author used the data from PVT-1⁵ to obtain the rate constant. The author regressed the loss-of-TPB⁻ data to the combined model (dual mechanism).

G value for radiolytic decomposition (G). The author used a G value of 2.1 molecules per 100 eV of energy deposited in the solids was. Appendix B describes the experiment that measured this G value.

Dose Rate. The calculations use the dose to the solids since the G value assumes that basis. To a first approximation, the dose to solids equals the total dose multiplied by the volume fraction of the solids. The solids typically settle or float until they reach approximately 5-7 vol % of the slurry. Since the beta decay energy comprises 80% of the total decay energy of Cs-137, and since it deposits very close to the decaying nucleus (located in the solid particles), a higher fraction of the beta energy is adsorbed than estimated from the volume percentage of the solids. Therefore, the author estimated the dose to solids as 10% of the total decay energy from Cs-137. The calculations ignore decay energy from other radioisotopes in the waste since their contribution is small compared to the preceding assumptions. For laboratory samples, the calculations assume only 10% of the beta energy is adsorbed since the majority of the gamma energy will escape the small containers used.

Initial NaTPB concentration. In all cases, the value for this parameter came from analytical measurements.

Radioactive Experiments

Figure 6 shows the model predictions for the radioactive experiments (Experiments 1 through 6). Table V lists the values for the model parameters.

For Experiments 1 and 2, the graphs show the change in potassium concentration with time. The model predicts the

general shape of the response, but typically predicts the amount of potassium in solution to be higher than observed experimentally. The discrepancy likely arises because the model assumes that the system is always at equilibrium. The simultaneous measurements of K^+ and TPB^- during the experiments do not match previously reported solubility products. The bias shows a lower K_{sp} consistent with slow dissolution of KTPB.

Experiment 3 showed a slow rate of loss of TPB^- , and significant changes in soluble potassium and cesium did not occur until late in the test. When one uses the observed rate of loss of TPB^- in the model ($k = .0025 \text{ h}^{-1}$), the model slightly under predicts the potassium concentration. However, since the potassium concentrations remain small, the differences probably lack significance.

Experiment 4 lacks potassium data due to dilution of the samples before analysis. Therefore, the author modeled the Cs-137 concentration changes. The model over predicts the Cs-137 concentration when using pure phase CsTPB solubility product. However, an excellent fit occurs when the Cs-137 solubility is reduced by a factor of 1/5. Previous solubility tests⁴ showed the apparent lower solubility of CsTPB when precipitated in the presence of KTPB and the observed bias (1/5) in this experiment falls within the expected range of this effect.

In Experiments 5 and 6, the model does not predict the general shape of the Cs-137 response. Decreasing the solubility for CsTPB makes the fit worse. Increasing the rate constant for decomposition of soluble TPB^- by an order of magnitude increases the predicted Cs-137 concentrations, but does not change the general shape of the curve. The lack of fit in these two experiments suggests another reaction pathway exists other than those included in the model.

Simulant Experiments

Figure 7 shows the model predictions for the simulant experiments (Experiments 7 through 12). Table V lists the values for the model parameters.

The model over predicts the soluble potassium concentrations in Experiments 7 and 8. The initial potassium and tetraphenylborate measurements for these experiments indicated high potassium and no tetraphenylborate in solution. At the next sampling, the potassium had precipitated, but little TPB^- was present. The TPB^- concentrations remained low and irregular. The data suggests that the excess NaTPB existed as a solid that slowly dissolved during the experiment. Since an additional source of NaTPB will suppress potassium and is not accounted for in the model, the model will over predict soluble potassium concentrations.

TABLE V. Parameter Values Used in Model Fitting

				Initial						
	Experiment	Temp.	[Na ⁺] (molar)	Solids (wt %)	NaTPB (mg/L)	K1	K2	k (h ⁻¹)	Dose Rate (eV/day)	Volume (gallons)
Real Waste	1	40	3.0	1.0	33	7.31E-09	9.54E-12	0.00009	4.40E+19	0.264
	2	40	3.0	4.0	363	7.31E-09	9.54E-12	0.0013	1.80E+20	0.264
	3	50	3.0	1.0	277	1.37E-09	1.61E-11	0.0016	4.40E+19	0.264
	4	50	3.0	4.0	129	1.37E-09	1.61E-11	0.018	1.80E+20	0.264
	5	65	0.5	4.0	629	2.69E-07	3.71E-10	0.04	1.80E+20	0.264
	6	65	1.5	4.0	525	1.67E-07	2.04E-10	0.04	1.80E+20	0.264
Simulant	7	40	3.0	4.0	50	7.31E-09	9.54E-12	0.0023	0	0.264
	8	40	3.0	4.0	50	7.31E-09	9.54E-12	0.0023	0	0.264
	9	40	3.0	4.0	251	7.31E-09	9.54E-12	0.0011	0	0.264
	10	40	3.0	4.0	366	7.31E-09	9.54E-12	0.00058	0	0.264
	11	50	3.0	4.0	231	1.37E-08	9.36E-11	0.0053	0	0.264
	12	70	3.0	4.0	96	4.84E-08	4.54E-11	0.014	0	0.264
Tank 48H	Post-1983	25	0.5		60,000	2.16E-08	4.63E-11	0.0025	5.22E+25	60,000
	Post-Batch#1	25	4.0		100	1.03E-09	1.46E-12	0.0025	1.04E+26	200,000
	PVT-1	25	3.0		60	2.84E-09	4.38E-12	0.0025	1.04E+26	250,000
Previous Tests*	Test#2	47	3.7	3.7	128	5.57E-09	6.30E-12	0.02	1.70E+20	0.264
	Test#4D	50	3.5	4.0	188	1.37E-08	1.60E-11	0.02	1.80E+20	0.264

*Reference1.

Since a low TPB⁻ concentration existed through most of the experiment, the soluble potassium never increased. Thus, the model assumption of equilibrium and the slow dissolution kinetics of NaTPB solids appear to explain why the model over predicts the potassium response in these experiments.

In Experiments 9 and 10, the concentration of TPB⁻ remained high throughout the tests and potassium never increased significantly. The model predicts this behavior when using the slow rate constant for decomposition of TPB⁻.

As with the higher temperature experiments with radioactive waste, the model does not accurately mimic the general shape of the response curve in Experiments 11 and 12. In Experiment 11 (50 °C), the model bounds the available experimental data, but the trend near the end of the test suggests that the experiment may exceed the model at longer duration. In Experiment 12 at 70 °C, the model never exceeds the observed response. Increasing the rate constant by an order of magnitude does not improve the fit significantly, suggesting a different mechanism at this higher temperature.

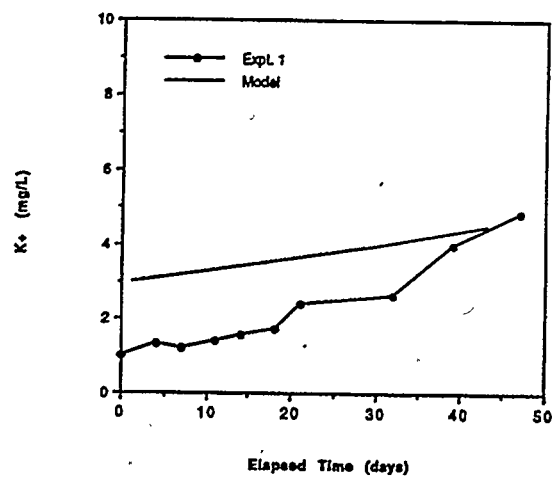
Tank 48H Data

Figure 8 shows the model predictions for Tank 48H following the 1983 ITP full-scale demonstration, 1995 Batch 1, and 1996 PVT-1 tests. Table V list the values for the model parameters.

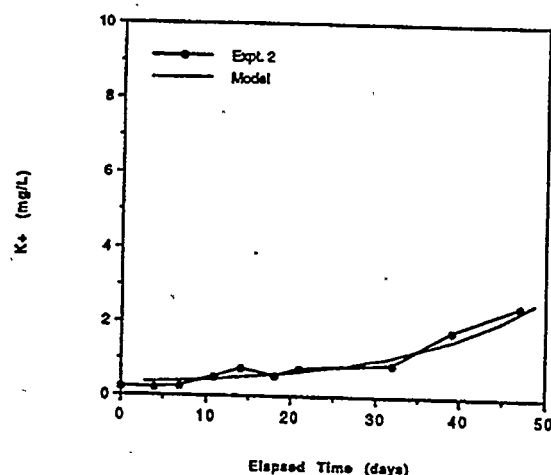
FIGURE 6. Model Results for Radioactive Experiments

Note: The vertical scales on these graphs are not all the same. Use care when comparing different experiments.

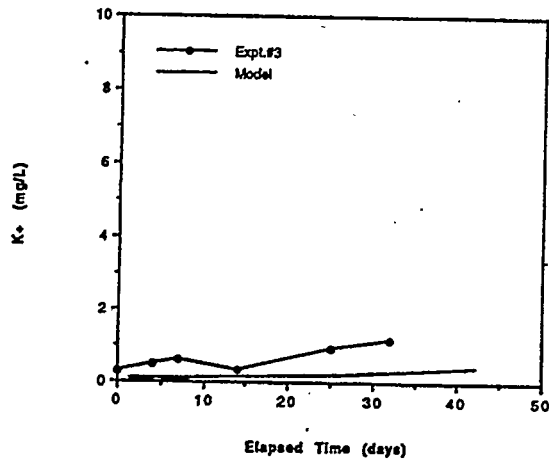
Experiment 1
(40 °C, 2.7 M Na⁺, 0.8 wt %)



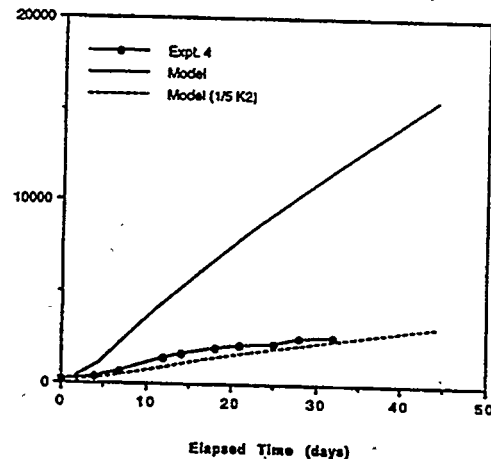
Experiment 2
(40 °C, 2.7 M Na⁺, 4.7 wt %)



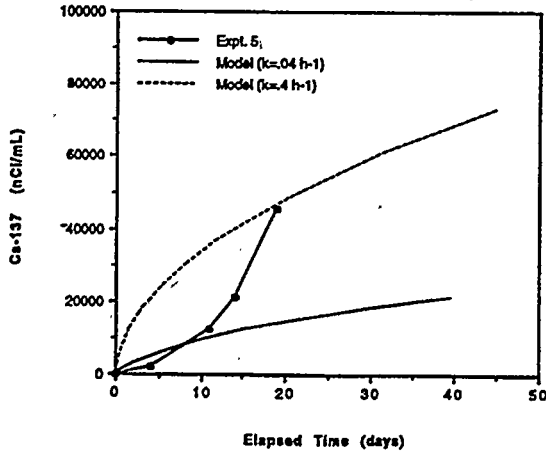
Experiment 3
(50 °C, 2.7 M Na⁺, 0.8 wt %)



Experiment 4
(50 °C, 2.7 M Na⁺, 4.7 wt %)



Experiment 5
(65 °C, 0.4 M Na⁺, 4.1 wt %)



Experiment 6
(65 °C, 0.9 M Na⁺, 4.8 wt %)

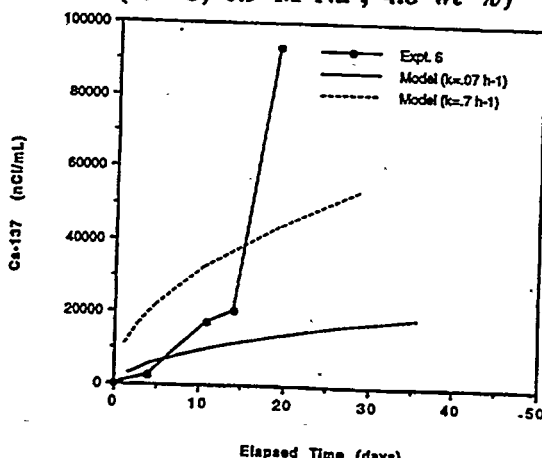
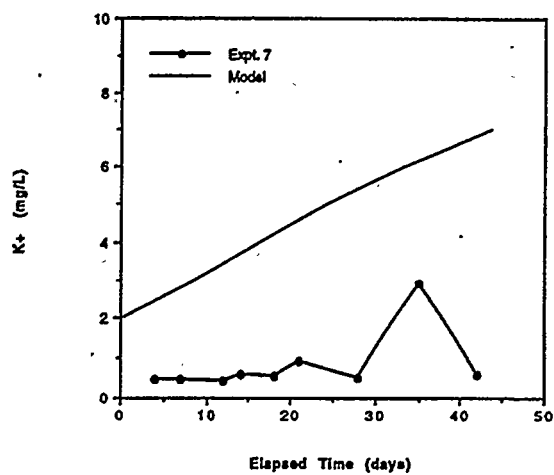


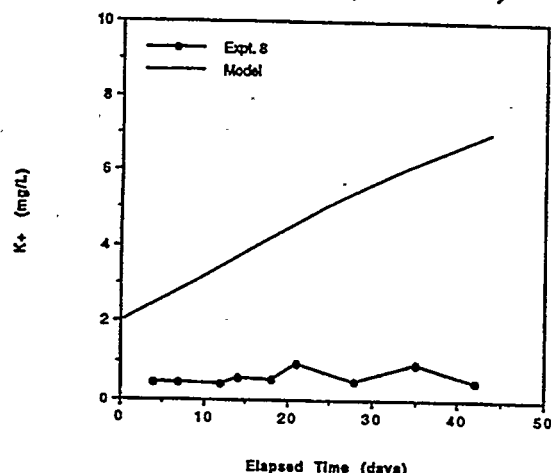
FIGURE 7. Model Results for Simulant Experiments

Notes: The vertical scales on these graphs are not all the same. Use care when comparing different experiments.

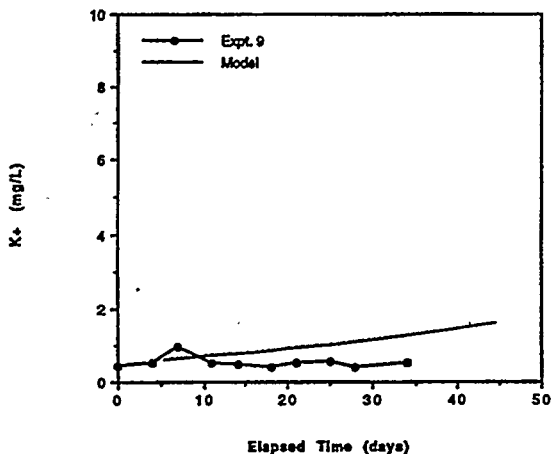
Experiment 7
(40 °C, 23.0 M Na⁺, 4.0 wt %)



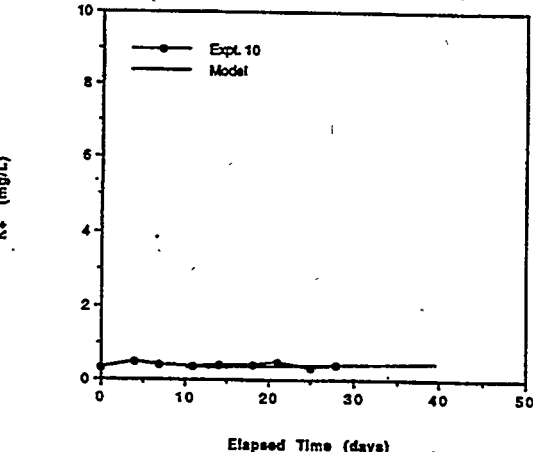
Experiment 8
(40 °C, 3.0 M Na⁺, 4.0 wt %)



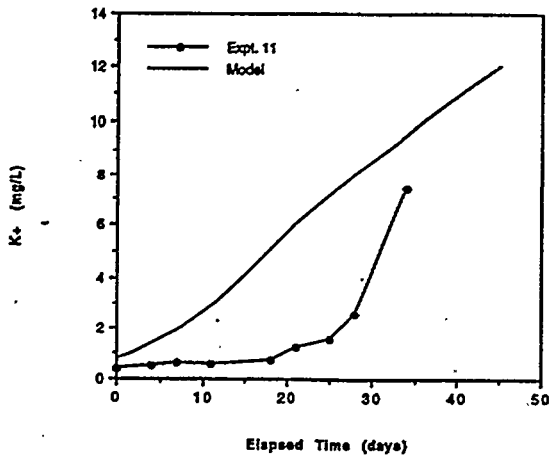
Experiment 9
(40 °C, 3.0 M Na⁺, 4.0 wt %)



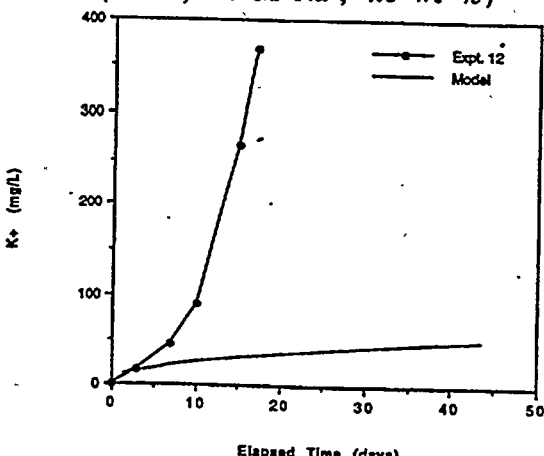
Experiment 10
(40 °C, 3.0 M Na⁺, 4.0 wt %)



Experiment 11
(49 °C, 3.0 M Na⁺, 4.0 wt %)



Experiment 12
(70 °C, 3.0 M Na⁺, 4.0 wt %)



The model over predicts the Cs-137 concentrations measured in Tank 48H following the 1983 ITP full-scale demonstration test when using the pure phase CsTPB solubility product.

Decreasing the solubility product by a factor of 1/3, dramatically improves the model fit to the data.

The model over predicts the Cs-137 concentration in Tank 48H for the time period from December 1995 to November 1996.

This may result from the slow dissolution of NaTPB solids from mixed crystal of (K,Na)TPB. A year after the addition of NaTPB for Batch 1 and just prior to the PVT-1 test in November 1996, the rate of increase in Cs-137 and potassium accelerated. The rate of increase in that time period began to approach the rate predicted from the model, suggesting consumption of all of the excess NaTPB. No significant changes in temperature, mixing, oxygen concentration, or slurry composition occurred that explain the change in rate just prior to PVT-1.

The model closely predicts the increase in potassium during and after PVT-1. Although the model over predicts the Cs-137 concentration when using the pure phase CsTPB solubility product, the prediction agrees with experimental results when the CsTPB solubility product is reduced to 1/3 the measured value.^{4,9} The current Tank 48H rate of increase in potassium is 0.16 mg/L/day (Figure 8). This corresponds to loss of 0.05 wt % KTPB solids per year. The model predicts that at low temperature when the catalytic mechanism is slow, the potassium rate is proportional to the radiation dose rate. Deviations due to slurry composition are possible but are expected to be small. These could be included in the model through changes in the G value or dose-to-solids calculation.

Previous Laboratory Tests

Figure 9 shows the model predictions for two experiments reported previously.¹ Table V lists the values for the model parameters for these experiments.

Test 2 of the previous study¹ used slurry from Tank 48H and intended to run at 40 °C. The actual temperature recorded during the first two days reached 45-47 °C, but decreased to an average of 38 °C afterwards. When predicted for 47 °C, the model does not reproduce the jump in Cs-137 found for the first day, nor does it fit the subsequent data (using either the pure phase CsTPB solubility product or a fraction of it). However, a good model fit results for the second and subsequent days if one uses a rate constant reflecting the lower temperature (40 °C) and reduces the pure phase CsTPB solubility by 50%. The jump in Cs-137 and potassium concentrations during the first day of the test are reproduced by the model if one assumes the rate constant is 0.2 to 0.4 h⁻¹. Previous tests measured rate constants of this magnitude but at higher temperatures (55°C) and higher

FIGURE 8. Model Results for Tank 48H

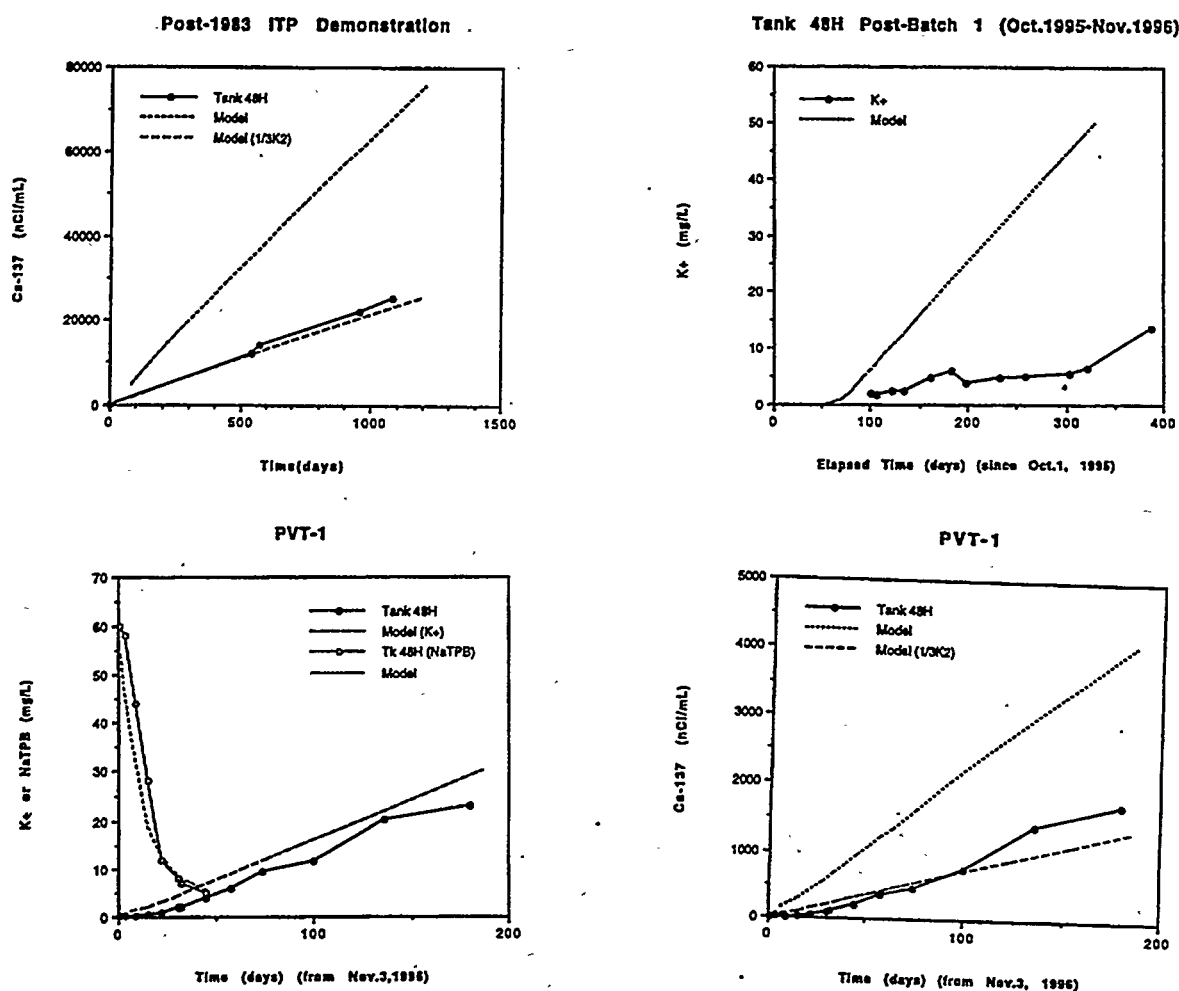
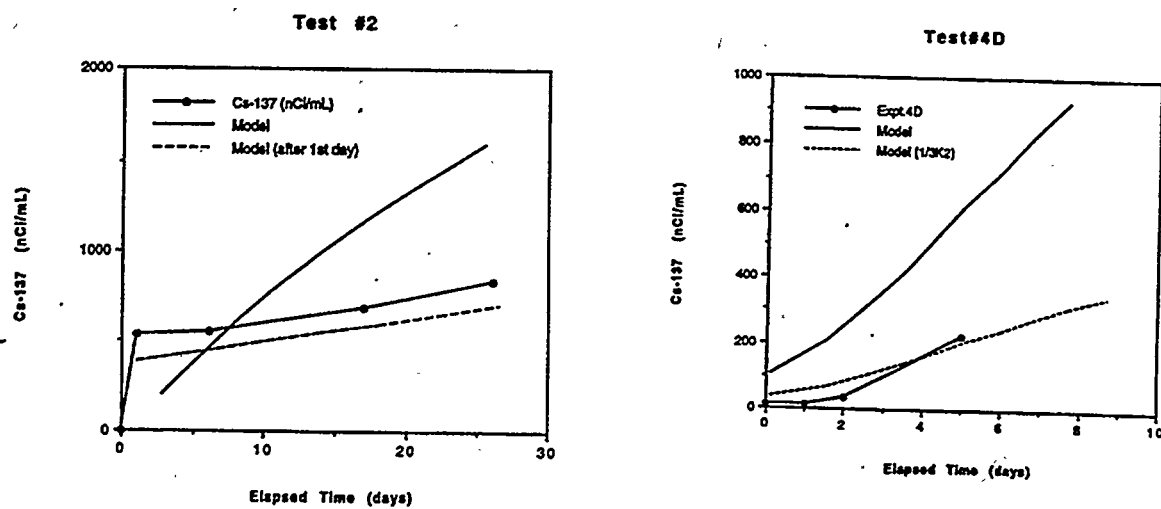


FIGURE 9. Model Results for Previous Laboratory Tests (Reference 1)



salt concentrations (4.7 M Na^+).⁸ Thus, the rate constant required to fit the model to the initial day's jump is an order of magnitude larger than expected. Also, if this large rate constant is used, the model greatly over predicts subsequent changes in Cs-137 concentrations.

The previous Test 4D used slurry from Tank 48H at 50 °C.¹ The increase in Cs-137 after the second day coincided with loss of the tetrphenylborate in solution. The model again over predicts the increase in Cs-137 when using the pure phase CsTPB solubility product, but agrees closely when the solubility product is reduced to 1/3 the measured value.

Discussion of Modeling Results

In general, the model works well at temperatures of 50 °C or below with the following observations.

- The model consistently over predicts Cs-137, but agrees well with experiments when K_{sp} for CsTPB is reduced to 1/2 to 1/5 of the pure phase value.

This discrepancy is within the variability of the solubility measurements on pure phase CsTPB ($\pm 69\%$).⁸ In addition, the systematic nature of the discrepancy suggests that it may arise from another source. The same behavior was detected in recent solubility measurements that indicate precipitation of CsTPB in the presence of KTPB lowers the apparent solubility of CsTPB.³⁻⁴ However, it could also arise from non-equilibrium conditions because of slow dissolution of CsTPB. Rates of dissolution of CsTPB have not been measured, so the cause of the discrepancy cannot be assessed.

- In several experiments, the model over predicts the potassium response.

This discrepancy likely results from the model assumption that the system remains at equilibrium relative to the solubility of KTPB, rather than from an error in the K_{sp} for KTPB. Slow dissolution kinetics for KTPB will cause results lower than predicted by the model.

Alternatively, slow dissolution of NaTPB solids may suppress the soluble potassium and cesium concentrations. In several experiments and Tank 48H the measured soluble NaTPB concentrations were less than expected ("missing" NaTPB). An additional source of NaTPB (such as slow dissolution of solids) will suppress potassium and Cs-137 concentrations compared to model predictions.

- The model does not predict the shape of the curve found in experiments at higher temperature.

This suggest that an additional reaction mechanism contributes significantly at the higher temperatures.

RECOMMENDATIONS FOR FURTHER TESTING

The results of the experiments and modeling suggest the following additional areas of investigation.

- Additional variable testing at low temperatures

The purpose of testing additional variables is to measure solids stability under a broader spectrum of conditions than was provided by the previous experiments. Future work should include a statistically designed set of experiments at 45 °C to study the following variables: salt concentration (0.1 to 5.5 molar), pH/OH⁻ (pH 10 to 3 M NaOH), continuous radiation (at 104 rad/h, similar to expected tank dose rates), total dose (to 200 Mrad), atmosphere (air and inerted), KTPB solids (2.5 and 5 wt %), and uranium (as a component of the catalyst system). Test durations should be adjusted to ensure that slow starting reactions have sufficient time to reach full velocity. These tests have been initiated.

- Scoping tests at higher temperatures

These tests are needed to define how much margin exists beyond the limits of the authorization basis. The primary purpose of these tests is to investigate the relationship between the threshold temperature and test duration for the high temperature reaction. In addition, an extended test could determine if the reaction is self-limiting or if all the available solids react. Measures of changes in other composition variables (products, organic intermediates, and soluble metals) could also help identify the mechanism of the reaction.

- G value measurements.

All modeling discussed above used a single G value for the radiolytic decomposition mechanism. The G values depend on the slurry composition and other factors. Measuring and using composition-dependent G values could improve the fit between the model and experimental data sets. In addition, these tests could investigate the importance of radiolytic destruction of soluble TPB⁻ (as opposed to solids). This additional mechanism may be important under conditions of low solids and high soluble TPB⁻ concentrations.

REFERENCES

1. D. D. Walker and C. A. Nash, "Results from Tank 48H Slurry Decontamination and Decomposition Experiments in Support of ITP Process Verification Testing (U)," WSRC-TR-96-0190, September 6, 1996.
2. D. D. Walker, M. J. Barnes, C. L. Crawford, R. F. Swingle, R. A. Peterson, M. S. Hay, and S. D. Fink, "Decomposition of Tetraphenylborate in Tank 48H (U)," WSRC-TR-96-0113, Rev.0, May, 10, 1996.
3. D. D. Walker, W. T. Boyce, C. J. Coleman, D. P. Diprete, T. B. Edwards, A. A. Ekechukwu, C. W. Hsu, S. F. Peterson, L. L. Tovo, and M. J. Whitaker, "Tank 48H Waste Composition and Results of Investigations of Analytical Methods (U)," WSRC-TR-97-0063, Rev.0, April 2, 1997.
4. M. S. Hay and D. J. McCabe, "Effect of the Potassium to Cesium Ratio on the Solubility of Cesium Tetraphenylborate (U)," WSRC-TR-97-0157, Rev.0; May 12, 1997.
5. D. D. Walker, W. T. Boyce, C. J. Coleman, D. P. Diprete, A. A. Ekechukwu, C. W. Hsu, S. F. Peterson, R. J. Ray, L. L. Tovo, M. J. Whitaker, and J. E. Young, "Analytical Results for Samples From Process Verification Test, Phase 1 (U)," WSRC-TR-97-0041, Rev.0, February 21, 1997.
6. R. E. Eibling, "The Potential for a Diphenylborinic Acid Reaction with Tetraphenylborate Anion in Aqueous Alkaline Solutions (U)." WSRC-TR-97-0147, May, 19, 1997.
7. M. J. Barnes, "Sodium Tetraphenylborate Catalyst Identification: Preliminary Studies Set 2 (U)," WSRC-TR-97-0144, Rev.0, May 28, 1997.
8. M. J. Barnes, C. L. Crawford, and C. A. Nash, "Sodium Tetraphenylborate Catalyst Identification: Preliminary Studies Set 1 (U)," WSRC-TR-97-0060, Rev.0, March 6, 1997.
9. D. J. McCabe, "Cesium, Potassium, and Sodium Tetraphenylborate Solubility in Salt Solution (U)," WSRC-TR-96-0384, Rev.0, December 16, 1996.
10. L. L. Tovo and W. T. Boyce, "Analysis of Copper in the In-Tank Precipitation Process Caustic Samples (U)," WSRC-TR-96-0400, December 12, 1996.
11. N. E. Bibler, "Calibration of Intense Co-60 Gamma Ray Sources at the Savannah River Plant," (U), DP-1414, May 1976.

APPENDIX A
Experimental

Preparation of Slurries

Tank 48H radioactive slurries

The radioactive slurries derived from a composite of the following samples from Tank 48H:

ITP-303 (6/16/96)	
ITP-304 (6/16/96)	
ITP-305 (6/16/96)	
ITP-306 (6/16/96)	ITP-350 (8/3/96)
ITP-332 (7/17/96)	ITP-351 (8/3/96)
ITP-333 (7/17/96)	ITP-352 (8/3/96)
ITP-339 (7/23/96)	ITP-353 (8/3/96)
ITP-340 (7/27/96)	ITP-362 (8/23/96)
ITP-341 (7/27/96)	ITP-363 (8/23/96)
ITP-342 (7/27/96)	ITP-364 (8/23/96)
ITP-346 (8/2/96)	ITP-366 (8/23/96)
ITP-347 (8/2/96)	ITP-367 (8/23/96)
ITP-349 (8/2/96)	ITP-368 (8/23/96)

The samples were combined in one bottle and the weight percentage solids measured ($2.43 \pm .02$ wt %). A portion of this slurry was set aside for dilution to 1 wt % solids. The remaining slurry was allowed to settle overnight and the clear supernate decanted to produce a 4.0 wt % slurry. Some of the supernate was added to the 2.4 wt % portion to produce a 1.03 wt % slurry. Portions of the 4 wt % slurry were removed and diluted with water to produce 0.5 and 1.5 molar Na^+ . Again, the solids were allowed to settle and the supernate decanted to produce 4.0 wt % solids slurries. The compositions of the slurries are listed in Table A-1.

Samples (20 g) of the undiluted slurries were placed in acetonitrile to dissolve the organic solids (KTPB and CsTPB). The solution was filtered and the insoluble residue washed with acetonitrile and acetone. The residues were dissolved in a mixture of concentrated hydrochloric (30 mL) and nitric (10 mL) acids by heating to 90 °C for one hour. The acid solution was diluted to 100 mL with water prior to analysis. The composition of the inorganic solids is listed in Table A-2.

Portions of the slurries (approximately 100 mL) were placed in polyethylene bottles and 1-3 mL of 0.1 molar sodium tetrphenylborate solution (Aldrich, ACS reagent grade, 99.5+% purity) added to achieve the target concentration. The amount of NaTPB added included enough to precipitate the initial free potassium ion (approx. 5 mg K^+/L). The slurries were stirred for one hour at ambient temperature (25-30°C), sampled, then placed in carbon steel containers (cylindrical).

TABLE A-1. Composition of Tank 48H Slurries

Experiment	1	2	3	4	5	6
Component	Concentration					
Na ⁺ (M)	2.7	2.7	2.7	2.7	0.39	0.90
NO ₂ ⁻ (M)	0.45	0.45	0.45	0.45	0.083	0.14
NO ₃ ⁻ (M)	0.35	0.35	0.35	0.35	0.057	0.10
OH ⁻ (M)	1.5	1.5	1.5	1.5	0.21	0.39
K ⁺ (mg/L)	1.0	<.2	0.3	3.4	1.2	0.9
NaTPB (mg/L)	33	363	277	129	629	525
3PB (mg/L)	39	54	23	34	10	21
2PB (mg/L)	<10	<10	<10	<10	<10	<10
1PB (mg/L)	<20	<20	<20	<20	51	25
phenol (mg/L)	1490	1540	1350	1350	590	250
Cu (mg/L)	0.54	0.54	0.54	0.54	0.30	0.47
Density (g/mL)	1.12	1.12	1.12	1.12	1.02	1.10
Solids (wt %)						
total*	0.8±.8	4.7±.1	0.8±.2	4.7±.1	4.1	4.8±.1
inorganic**	0.34±.04	0.9±.2	0.34±.04	0.9±.2	(0.8)†	(0.9)†

*Filterable solids insoluble in water.

**Filtered solids insoluble in water, acetonitrile, and acetone.

†Values in parentheses estimated based on other analyses.

TABLE A-2. Composition of Inorganic Solids in Tank 48H Slurries

Experiment	1	2
Component	Concentration*	
	(wt % of inorganic solids)	
Fe	1.0	1.0
Al	2.5	4.9
Si	1.4	1.4
Ca	.28	.41
Cr	.15	.14
Mg	.36	.30
Mn	.14	.10
Cu	.02	<.01
Ti	15.6	12.0

*Weight percentage of the dried inorganic solids that were insoluble in acetonitrile and acetone.

4 cm diameter, 12 cm tall, 150 mL internal volume). A top plate containing a septum port was bolted to the cylindrical vessel using a Teflon washer as a seal. The vessels were placed in ovens at the required temperatures. Samples of slurry were removed from the vessel by inserting a stainless steel needle through silicone rubber septa in the ports on the lids. The samples (approximately 8 mL) were filtered using disposable nitrocellulose filters (0.45 micron nominal pore size). The filtrate was analyzed for Cs-137 activity, potassium ion, NaTPB, 3PB, 2PB, 1PB, and phenol.

Simulated Slurries

Experiment 7. A simulated slurry was prepared with the composition shown in Table A-3. The KTPB was precipitated in the presence of a low sodium ion concentration and the soluble sodium salts were added after precipitation. The components of the catalyst system were added next (Table A-4). The slurry was then irradiated to a dose of 5.0 Mrad at a dose rate of 1.5E6 rad/h. After irradiation, NaTPB was added to produce 1.7 wt % NaTPB solids in the slurry. The slurry was then heated to 70 °C for 25 days to decompose the excess NaTPB and produce decomposition compounds. After 25 days, a portion of slurry (5.6 g) was diluted with water (10 g) and stirred for 30 minutes. It was then filtered and the filtrate analyzed for NaTPB (found: 800 mg/L). The result indicated the undiluted slurry contained 2400 mg NaTPB/L, or about 14% of the original amount (86% decomposed).

After the initial 25-day incubation period, a portion of the slurry (100 mL) placed in a 160-mL glass serum vial and sealed with a Teflon coated septum. The slurry was returned to the oven at 70 °C and incubated without stirring. The vial was sampled every three or four days using a syringe and needle. The samples were filtered and the filtrate analyzed for potassium, NaTPB, 3PB, 2PB, 1PB, and phenol.

Experiments 8 and 9. The slurry prepared for Experiment 7 was used in these experiments. After the 25-day decomposition period, potassium (0.20 g KNO₃) was added to a portion of the slurry (220 mL) to precipitate the remaining NaTPB. The amount of potassium added was based on the analysis for NaTPB described above. The slurry was stirred for 4 days at room temperature (approximately 23 °C) and a portion filtered. The filtrate contained 236 mg potassium per liter which was much higher than expected since it should have been precipitated by the excess NaTPB. Although the NaTPB was present in the slurry as a solid, the conversion reaction to KTPB was slow and was only 40% complete after four days of stirring. The slurry was split into two 100 milliliter portions and different amounts of NaTPB were added to each (Experiment 8, 0.075 mmole; Experiment 9, 0.15

mmoles). These amounts should have produced approximately 200 and 400 mg of soluble NaTPB per liter in the two experiments. However, due to the slow conversion of the NaTPB solids to KTPB solids, the initial test samples contained excess K⁺.

The two portions of slurry were placed in 160-mL glass serum vials, sealed with Teflon coated septa, and the airspace purged with nitrogen for 5 minutes. The vials were placed in a thermostated oven at 40 °C. The samples were not stirred except prior to sampling. The vials were sampled every three or four days by removing the serum cap and taking an 8-mL portion via pipette. The vials were recapped, purged with nitrogen, and returned to the oven. The samples were filtered and the filtrate analyzed for potassium, NaTPB, 3PB, 2PB, 1PB, and phenol.

Experiment 10,11, and 12. A slurry with the same composition as Experiment 7 (Table A-3) with the same catalyst additives (Table A-4) was prepared for Experiment 10. The slurry was irradiated to a dose of 5 Mrad at a dose rate of 1.9E5 rad/h. The irradiated slurry contained 0.7 mg soluble K⁺ per liter and 42 mg soluble NaTPB per liter. The slurry was divided into three portions (135 mL each) and NaTPB was added. The target NaTPB concentrations were 200 mg/L (Experiments 10 and 12) and 400 mg/L (Experiment 11). The three portions of slurry were placed in 160-mL glass serum vials, sealed with Teflon coated septa, and the airspace purged with nitrogen for 5 minutes. The vials were placed in ovens at 40 °C (Experiment 10 and 11) and at 50 °C (Experiment 12). The slurries were not stirred except prior to sampling. The vials were sampled every three or four days by removing the serum cap and taking an 8-mL portion via pipette. The vials were recapped, purged with nitrogen, and returned to the oven. The samples were filtered and the filtrate analyzed for potassium, NaTPB, 3PB, 2PB, 1PB, and phenol.

TABLE A-3. Simulant Slurry Composition

<u>Component</u>	<u>Concentration</u>
KTPB	4.0 wt %
Na ⁺	3.0 M
OH ⁻	1.7 M
NO ₂ ⁻	0.45 M
NO ₃ ²⁻	0.44 M
CO ₃ ²⁻	0.12 M
SO ₄ ²⁻	0.004 M
Cl ⁻	0.009 M
F ⁻	0.005 M
PO ₄ ³⁻	0.005 M

TABLE A-4. Catalyst Components in Simulant Experiments

Insoluble Components (wt % of slurry)

0.2 wt % sludge

0.2 wt % monosodium titanate

Sludge composition:

Component	Concentration (wt % of dry sludge)	Component	Concentration (wt % of dry sludge)
Al	4.8	Cu	0.1
Fe	18.8	Mg	0.1
Mn	5.9	Ni	2.5
Ru	0.23	Pb	0.3
Pd	0.11	Zn	0.2
Rh	0.06	Zr	2.5
Cr	0.2		

Metal Additives (mg/L)

Cu(II)	1.7	Ru(III)	0.8
Mo(VI)	12.	Pd(II)	0.4
Cr(VI)	60.	Rh(III)	0.2
Si(IV)	16	Ag(I)	0.6
Cd(II)	0.4	Co(II)	0.04
Se(VI)	1	Hg(II)	2.2
As(IV)	0.04	Ca(II)	12.2
Zn(II)	8.8	Sr(II)	0.1
Pb(II)	1.2	La(III)	0.05
Fe(III)	2.6	Ce(IV)	0.3
Sn(III)	2.1		

Organic Additives (mg/L)

Diphenylmercury 150

Temperature Control

The range and average temperatures during the experiments are listed in Table A-1. For experiments with radioactive slurries at 40 and 50°C, the oven temperatures were continuously monitored with a thermocouple device and recorded on a circular chart. In addition, daily readings also recorded by operators. For Experiments 5 and 6 at 65°C, the temperature was automatically recorded every 30 minutes. For simulant experiments, the temperature from a Hg/glass thermometer and thermocouple were recorded daily by an operator. The average of daily temperatures are listed in Table A-5.

The temperatures were maintained within ± 4 °C of the desired temperatures at all times except when taking samples and except for one episode during Experiments 3 and 4. The

TABLE A-5 Average and Range of Temperatures During Experiments 1 through 12

<u>Experiment</u>	Temperatures (°C)		
	<u>Target</u>	<u>Average</u>	<u>Range*</u>
1, 2	40	40	38-42
3, 4	50	50	44-64
5, 6	65	64	64-65
7, 8, 9, 10	40	40	39-43
11	50	49	45-52
12	70	70	67-73

*Excluding sampling events.

temperature set point on the oven used in Experiments 3 and 4 was inadvertently moved four days into the test. The temperature dropped to 44 °C for 15 hours. It was then overcorrected to 64 °C for 3 hours before it was correctly adjusted to 50 °C. Based on the results for the samples taken before and after the temperature excursion, there does not appear to have been any adverse effect. The temperature was maintained in the range 47 to 52 °C for the remaining 37 days of the experiment.

Analytical Results

The analytical results for the filtrate samples from all experiments are listed in Tables A-6 to A-17.

Analytical Methods

The following analyses were performed by the Analytical Development Section of SRTC.

Cs-137 was measured by gamma spectroscopy counting methods using 3 mL samples. A high-purity germanium gamma spectroscopy system operated through a Canberra Genie PC software interface was used for the analysis. The method is described in Manual L16.1, Procedure #ADS-2420.

Phenylboronic acid (1PB) and phenol were measured by high performance liquid chromatography (HPLC) on a Hewlett Packard LC with a 2.1x250 mm Dychrom Chemosorb 5-ODS-UH column using acetonitrile-water eluent. The HPLC instrument methods are described in Manual L16.1, Procedure #ADS-2655. The methodology of sample preparation, standards, and standard preparation for HPLC analyses is described in SRT-ADS-96-0438.

Potassium and sodium ion concentrations were measured by flame atomic absorption using a Varian SpectrAA-400 spectrometer. Each sample is diluted 1:4 (sample:suppressant) in a suppressant solution of 2000 µg/mL cesium. For more

TABLE A-6. Analytical Results for Experiment 1

Elapsed Time (days)	Cs-137 (nCi/mL)	K ⁺ (mg/L)	NaTPB (mg/L)	3PB (mg/L)	2PB (mg/L)	1PB (mg/L)	Phenol (mg/L)
0	15.2	1.0	33	39	<10	<20	1343
4	32.9	1.3	<10	35	<10	<20	1493
7	28.2	1.2	<10	30	9	<20	1343
11	37.2	1.4	<10	39	<10	<20	1326
14	44.5	1.6	32	41	<10	<15	1374
18	54.3	1.7	18	45	<10	<20	1308
21	83.5	2.4	18	24	<10	<20	1302
32	89.1	2.6	13	14	<10	<20	1441
39	202	4.0	11	5	<10	<20	1432
47	286	4.8	7	34	5	<20	1343

TABLE A-7. Analytical Results for Experiment 2

Elapsed Time (days)	Cs-137 (nCi/mL)	K ⁺ (mg/L)	NaTPB (mg/L)	3PB (mg/L)	2PB (mg/L)	1PB (mg/L)	Phenol (mg/L)
0	0.9	<.2	363	54	<10	<20	1343
4	1.3	<.2	243	48	<10	<20	1536
7	0.8	0.2	243	52	<10	<20	1343
11	2.3	0.5	234	73	14	<20	1341
14	2.3	0.7	199	81	12	<15	1299
18	3.0	0.5	158	90	14	20	1359
21	4.6	0.7	137	96	10	18	1388
32	6.2	0.8	78	109	<10	153	1001
39	70.	1.7	27	134	10	35	1563
47	116.	2.4	10	115	6	<20	1543

TABLE A-8. Analytical Results for Experiment 3

Elapsed Time (days)	Cs-137 (nCi/mL)	K ⁺ (mg/L)	NaTPB (mg/L)	3PB (mg/L)	2PB (mg/L)	1PB (mg/L)	Phenol (mg/L)
0	24.	0.3	277	23	<10	<20	1350
4	8.0	0.5	249	65	<10	13	1286
7	7.8	--*	280	--	--	--	1410
12	6.0	--*	NR**	NR	NR	NR	NR
14	10.9	0.3	160	87	<10	141	1374
25	20.6	0.9	86	98	<10	<20	1440
32	26.6	1.2	114	92	<10	23	1520
42	55.9	3.4	16	95	<10	22	1614

*Due to dilutions of these samples, the resulting measurements were too close to or below detection limits to produce usable data.

** NR indicates the analysis was not requested.

TABLE A-9. Analytical Results for Experiment 4

Elapsed Time (days)	Cs-137 (nCi/mL)	K ⁺ (mg/L)	NaTPB (mg/L)	3PB (mg/L)	2PB (mg/L)	1PB (mg/L)	Phenol (mg/L)
0	160	3.4	129	34	<10	<20	1351
4	340	4.6	14	60	<10	14	1299
7	680	--*	--	--	--	--	1410
12	1330	--	--	--	--	--	--
14	1580	--	--	--	--	--	--
18	1900	--	--	--	--	--	--
21	2100	--	--	--	--	--	--
25	2140	--	--	--	--	--	--
28	2500	--	--	--	--	--	--
32	2540	--	--	--	--	--	--

*Due to dilutions of these samples, the resulting measurements were too close to or below detection limits to produce usable data.

TABLE A-10. Analytical Results for Experiment 5

Elapsed Time (days)	Cs-137 (nCi/mL)	K ⁺ (mg/L)	NaTPB (mg/L)	3PB (mg/L)	2PB (mg/L)	1PB (mg/L)	Phenol (mg/L)
0	34.	1.2	629	10	<10	51	590
4	2080	39.1	18	507	185	<20	545
11	12,400	152	<10	392	470	165	393
14	21,200	196	<10	315	517	237	432
19	45,300	480	NR	NR	NR	NR	NR

*NR indicates the analysis was not requested.

TABLE A-11. Analytical Results for Experiment 6

Elapsed Time (days)	Cs-137 (nCi/mL)	K ⁺ (mg/L)	NaTPB (mg/L)	3PB (mg/L)	2PB (mg/L)	1PB (mg/L)	Phenol (mg/L)
0	13.	0.87	525	21	<10	35	251
4	2310	38.2	<10	406	143	<20	214
11	17,100	176	<10	308	341	229	749
14	20,500	227	<10	253	262	239	838
19	93,300	860	NR	NR	NR	NR	NR

*NR indicates the analysis was not requested.

TABLE A-12. Analytical Results for Experiment 7

Elapsed Time (days)	K ⁺ (mg/L)	NaTPB (mg/L)	3PB (mg/L)	2PB (mg/L)	1PB (mg/L)	Phenol (mg/L)
0	176.	<10	900	1030	2710	2060
4	0.5	28	710	820	2290	2550
7	0.5	36	690	715	2050	2330
12	0.4	24	540	720	2190	2580
14	0.6	21	440	670	1960	2300
18	0.6	20	350	610	2020	2690
21	0.9	<10	260	290	1950	2630
28	0.5	<10	130	420	1590	3060
35	2.9	<10	63	173	1010	3230
42	0.6	<10	37	60	490	3480

TABLE A-13. Analytical Results for Experiment 8

Elapsed Time (days)	K ⁺ (mg/L)	NaTPB (mg/L)	3PB (mg/L)	2PB (mg/L)	1PB (mg/L)	Phenol (mg/L)
0	163.	<10	880	1020	2680	2050
4	0.5	34	750	750	2220	2560
7	0.4	45	820	670	2030	3040
12	0.4	27	630	630	2040	2860
14	0.6	23	530	600	1870	2540
18	0.6	26	440	520	1820	2810
21	1.0	48	380	460	1830	2780
28	0.5	<10	210	320	1270	3210
35	0.9	<10	140	89	620	3590
42	0.5	<10	123	<10	220	3710

TABLE A-14. Analytical Results for Experiment 9

Elapsed Time (days)	K ⁺ (mg/L)	NaTPB (mg/L)	3PB (mg/L)	2PB (mg/L)	1PB (mg/L)	Phenol (mg/L)
0	0.4	250	13	210	53	36
4	0.5	190	12	23	107	71
7	1.0	<10	16	67	160	100
11	0.5	200	18	36	71	121
14	0.5	210	23	18	99	143
18	0.4	180	23	<10	148	154
21	0.5	180	34	<10	28	167
25	0.5	140	27	<10	33	186
28	0.4	130	29	<10	28	189
34	0.5	120	28	<10	<20	192
41	0.7	67	29	<10	<20	220

TABLE A-15. Analytical Results for Experiment 10

Elapsed Time (days)	K ⁺ (mg/L)	NaTPB (mg/L)	3PB (mg/L)	2PB (mg/L)	1PB (mg/L)	Phenol (mg/L)
0	0.3	370	12	210	69	42
4	0.5	330	18	122	107	73
7	0.4	360	16	66	177	100
11	0.3	340	20	33	68	115
14	0.4	330	21	18	144	147
18	0.4	320	23	<10	42	169
21	0.4	280	35	<10	31	176
25	0.5	290	24	<10	46	185
28	0.3	260	27	<10	30	198
34	0.4	250	27	<10	19	198
41	0.6	190	35	<10	<20	243

TABLE A-16. Analytical Results for Experiment 11

Elapsed Time (days)	K ⁺ (mg/L)	NaTPB (mg/L)	3PB (mg/L)	2PB (mg/L)	1PB (mg/L)	Phenol (mg/L)
0	0.4	230	13	210	61	41
4	0.5	240	16	48	147	102
7	0.6	200	41	13	141	129
11	0.6	93	60	9	39	143
14	<0.1	77	59	<10	66	164
18	0.7	53	49	<10	16	169
21	1.2	34	55	55	<20	180
25	1.6	19	46	<10	<20	195
28	2.6	<10	45	<10	<20	212
34	7.4	3	39	<10	<20	198
41	22.6	10	28	<10	<20	240

TABLE A-17. Analytical Results for Experiment 12

Elapsed Time (days)	K ⁺ (mg/L)	NaTPB (mg/L)	3PB (mg/L)	2PB (mg/L)	1PB (mg/L)	Phenol. (mg/L)
0	0.34	96	520	650	2700	1050
3	15.3	101	220	200	2030	1190
7	44.6	8	15	52	1070	1340
10	91.1	<10	<10	24	490	1640
15	268.	<10	<10	<10	40	1830
17	368.	<10	<10	<10	31	1740

concentrated samples, additional dilutions are made with 1600 $\mu\text{g/mL}$ cesium. The method is described in Manual L16.1, Procedure #ADS-1549.

Boron and aluminum concentrations were measured by Inductively Coupled Plasma Emission Spectroscopy (ICPES) using an ARL 3580 instrument.

Copper concentrations were measured by Inductively Coupled Plasma Emission Spectroscopy (ICPES) using an ARL 3580 instrument. Samples were diluted 10X and acidified to a pH less than or equal to 2 using 5 wt % nitric acid. Spiked samples were analyzed with each sample to verify that there is no loss of copper. A 1000 mg/L copper standard purchased from High Purity, Inc. was used to prepare the spikes. The method is described in Manual L16.1, Procedure #ADS-1509 and in Reference 10.

Nitrate and nitrite concentrations were determined using ion chromatography. Samples were diluted to within linear calibration range (1-40 ppm) and eluted from a low capacity ion exchange resin column (AG4A/AS4A, Dionex) using carbonate/bicarbonate eluent. The instrument used was a Dionex Series 2000 Advanced Chromatography System with isocratic elution and conductivity detection. The method is described in Manual L16.1, Procedure #ADS-2306.

Free hydroxide was measured by titration with 0.1 N HCl using a Radiometer VIT90 Autotitration System. The sample was first saturated with strontium chloride to precipitate the carbonate. The hydroxide was then measured by titration to an endpoint of pH 4. The method is described in Manual L16.1, Procedure #ADS-2256.

Weight percentage solids were measured by gravimetric methods in the Shielded Cells. A slurry sample (5-10 g) was filtered through a preweighed filter paper (Whatman, fiberglass, 0.45 micron, 5.5 cm diameter), the solids washed with three 5 mL portions of water, and the filter paper dried to constant weight at 100 °C.

Dose rates in Co-60 gamma sources were measured with nylon film dosimeters.¹¹

APPENDIX B
G Value for Appearance of K⁺ from Radiolysis

The G value for appearance of potassium in solution following irradiation was measured on a simulated slurry with the composition shown in Table B-1. Portions (30 mL) of this slurry were sealed in glass serum vials and irradiated in a Co-60 gamma source to doses of up to 92 Mrad. Duplicate samples were prepared at each total dose. The dose rate varied between 4.3×10^5 to 6.7×10^5 rad/h depending on the position in the source. Following irradiation, the samples were stirred for periods of one week or two weeks to allow equilibration of K⁺ in solution. After stirring, the samples were filtered through 0.45 micron nitrocellulose disposable filters and the filtrate analyzed for K⁺ by atomic absorption spectroscopy. The results of the analyses are listed in Table B-2 and graphed in Figure B-1. No consistent bias was found between the sets stirred for one week and two weeks before analysis, indicating that potassium equilibration between the solution and solids is either very rapid (<<1 week) or very slow (>>2 weeks).

The G value for potassium appearance is calculated from the slope of the line in Figure B-1. The calculation based on the dose to the entire slurry is:

$$\left(\frac{3.76 \text{ mg/L}}{1 \times 10^6 \text{ rad}} \right) \left(\frac{1 \text{ rad}}{6.24 \times 10^{13} \text{ eV/g}} \right) \left(\frac{6.022 \times 10^{23} \text{ atoms K}^+}{39100 \text{ mg}} \right) \left(\frac{1 \text{ L}}{1120 \text{ g}} \right) = \\ = .083 \text{ molecules/100 eV (dose to slurry).}$$

To apply the results of this experiment to other slurries at different weight percentage solids, this G value can be adjusted based on the dose to solids. The electron densities in the solids and solution are similar, so the deposited radiation energy is assumed to be distributed between solids and slurry based on the weight fraction of each. The G value for dose to solids is:

$$.083/.04 = 2.1 \text{ molecules/100 eV (dose to solids).}$$

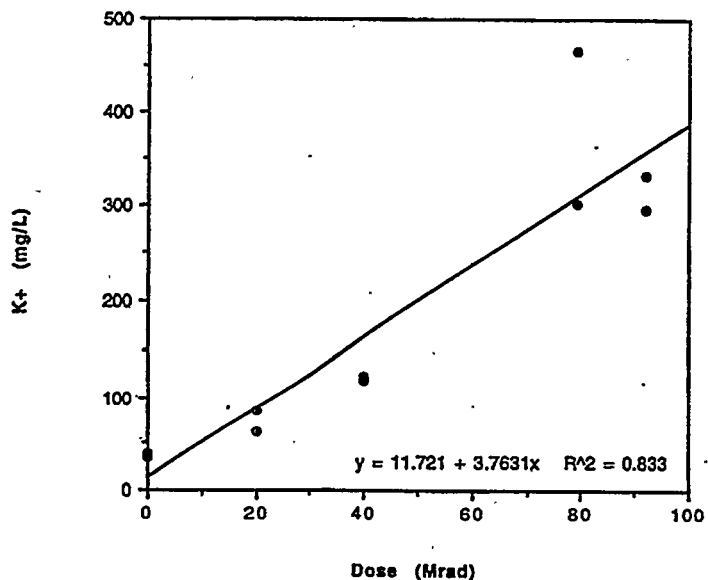
Table B-1. Composition of Simulated Slurry for G Value Measurement

<u>Component</u>	<u>Concentration (molar)</u>
OH ⁻	1.5
NO ₃ ⁻	0.45
NO ₂ ⁻	0.45
CO ₃ ²⁻	0.25
SO ₄ ²⁻	0.05
Total Na ⁺	3.0
KTPB solids	4.0 wt %

Table B-2. Potassium Concentrations After Radiolysis

<u>Dose (Mrad)</u>	<u>Potassium Concentration (mg/L)</u>	<u>After 1 week</u>	<u>After 2 weeks</u>
0	37		33
20.0	62		85
40.1	120		123
79.2	467		303
92.0	296		332

Figure B-1. Potassium Concentrations After Radiolysis



APPENDIX C
Calculation of K_1 and K_2 for Decomposition Model

Values for K_1 and K_2 at different temperatures and ionic strength are listed in Table C-1. K_1 and K_2 are related to the solubility products for KTPB and CsTPB by the following equations.

$$\text{KTPB: } K_1 = \frac{K_{sp}(\text{KTPB})}{\gamma_{K^+} \gamma_{\text{TPB}^-}}$$

$$\text{CsTPB: } K_2 = \frac{K_{sp}(\text{CsTPB})}{\gamma_{\text{Cs}^+} \gamma_{\text{TPB}^-}}$$

The temperature dependence of the solubility products between 25 and 65 °C are given by the following equations from Reference 10.

$$K_{sp}(\text{KTPB}) = 7.81\text{E-}9 e^{0.063T}$$

$$K_{sp}(\text{CsTPB}) = 2.328\text{E-}11 e^{0.05199T}$$

where T is the temperature in degrees Centigrade.

The solubility products are defined by the following equations.

$$K_{sp}(\text{KTPB}) = [K^+] [\text{TPB}^-] \gamma_{K^+} \gamma_{\text{TPB}^-}$$

$$K_{sp}(\text{CsTPB}) = [\text{Cs}^+] [\text{TPB}^-] \gamma_{\text{Cs}^+} \gamma_{\text{TPB}^-}$$

The activity coefficients (γ_{K^+} , γ_{Cs^+} , and γ_{TPB^-}) depend on the ionic strength of the solution and are calculated from the following equations.

$$\gamma_{K^+} = 0.284I_m^2 - 0.219I_m + 0.777$$

$$\gamma_{\text{Cs}^+} = 0.258I_m^2 - 0.160I_m + 0.783$$

$$\gamma_{\text{TPB}^-} = 1.91I_m^3 - 4.54I_m^2 + 5.48I_m + 0.712$$

The ionic strength (I_m) is calculated from the following equation.

$$I_m = 0.5[(z_a^2 m_a) + (z_b^2 m_b) + (z_c^2 m_c) + \dots]$$

where z_x = charge on ion x in solution

m_x = molal concentration of ion x (moles/1000 g solvent)

The density of the salt solutions in Tank 48H and in the simulants is given by the following equation.¹¹

$$\rho \text{ (g/mL)} = 1.0045 + 0.03899[\text{Na}^+]$$

where $[\text{Na}^+]$ is the total sodium ion concentration (moles/L)

Table C-1. Values for K_1 (KTPB) and K_2 (CsTPB)

K_1 (KTPB)

[Na ⁺] (molar)	25	40	47	Temperature (°C)		
				50	65	70
0.5	2.16E-8	5.56E-8		1.04E-7	2.69E-7	3.68E-7
1.5	1.34E-8	3.45E-8		6.47E-8	1.67E-7	2.28E-7
3.0	2.84E-9	7.31E-9		1.37E-8	3.53E-8	4.84E-8
3.7		3.59E-9	5.57E-9			
4.0	1.03E-9	2.66E-9		4.99E-9	1.28E-8	1.76E-8
4.7	5.12E-10	1.32E-9		2.48E-9	6.38E-9	8.74E-9
5.0	3.80E-10	9.78E-10		1.84E-9	4.73E-9	6.48E-9

K_2 (CsTPB)

[Na ⁺] (molar)	25	40	47	Temperature (°C)		
				50	65	70
0.5	4.63E-11	1.01E-10		1.70E-10	3.71E-10	4.81E-10
1.5	2.55E-11	5.57E-11		9.36E-11	2.04E-10	2.65E-10
3.0	4.38E-12	9.54E-12		1.61E-11	3.50E-11	4.54E-11
3.7		4.38E-12	6.39E-12			
4.0	1.46E-12	3.19E-12		5.37E-12	1.17E-11	1.52E-11
4.7	7.26E-13	1.58E-12		2.66E-12	5.81E-12	7.54E-12
5.0	5.45E-13	1.19E-12		2.00E-12	4.36E-12	5.65E-12

Keywords: In-Tank Process, Benzene

Retention: Permanent

CC: D. B. Amerine, 719-4A
K. Andringa, 773-41A
J. L. Barnes, 704-S
M. J. Barnes, 773-A
T. E. Britt, 732-B
B. T. Butcher, 773-43A
J. T. Carter, 704-25S
G. L. Cauthen, 241-119H
W. C. Clark, 704-56H
C. L. Crawford, 773-41A
D. E. Doughty, 704-56H
L. O. Dworjanyn, 779-2A
S. J. Eberlein, 704-56H
H. H. Elder, 704-S
T. J. Fiske, 241-120H
J. R. Fowler, 704-Z
F. R. Graham, 773-A
M. S. Hay, 773-A
M. J. Hitchler, 730-2B
D. T. Hobbs, 773-A
E. W. Holtzscheiter, 773-A
R. A. Jacobs, 704-T
M. D. Johnson, 704-56H
M. T. Keefer, 704-56H
L. F. Landon, 704-T
T. J. Lex, 719-4A
L. S. Livingston, 703-H
P. E. Lowe, 773-41A
J. C. Marek, 704-T
D. J. McCabe, 773-43A
J. W. McCullough, 703-H
J. D. Menna, 730-2B
M. S. Miller, 704-56H
M. J. Montini, 704-56H
J. P. Morin, 719-4A
C. A. Nash, 676-1T
L. M. Nelson, 773-43A
L. M. Papouchado, 773-A
S. F. Piccolo, 704-56H
R. A. Peterson, 773-41A
C. T. Randall, 704-T
P. L. Rutland, 242-152H
R. M. Satterfield, 719-4A
W. E. Stevens, 773-A
P. C. Suggs, 703-H
R. F. Swingle, 773-A
W. L. Tamosaitis, 773-A
M. C. Thompson, 773-A
W. B. VanPelt, 676-1T
D. D. Walker, 773-A
A. W. Wiggins, 241-152H
W. R. Wilmarth, 773-42A
A. L. Wooten, 732-B
G. T. Wright, 773-A
TIM, 703-43A
LWP Files c/o A. Patterson, 773-A
ITP Files c/o A.G. Wiest, 241-119H